Test Report No. 620841

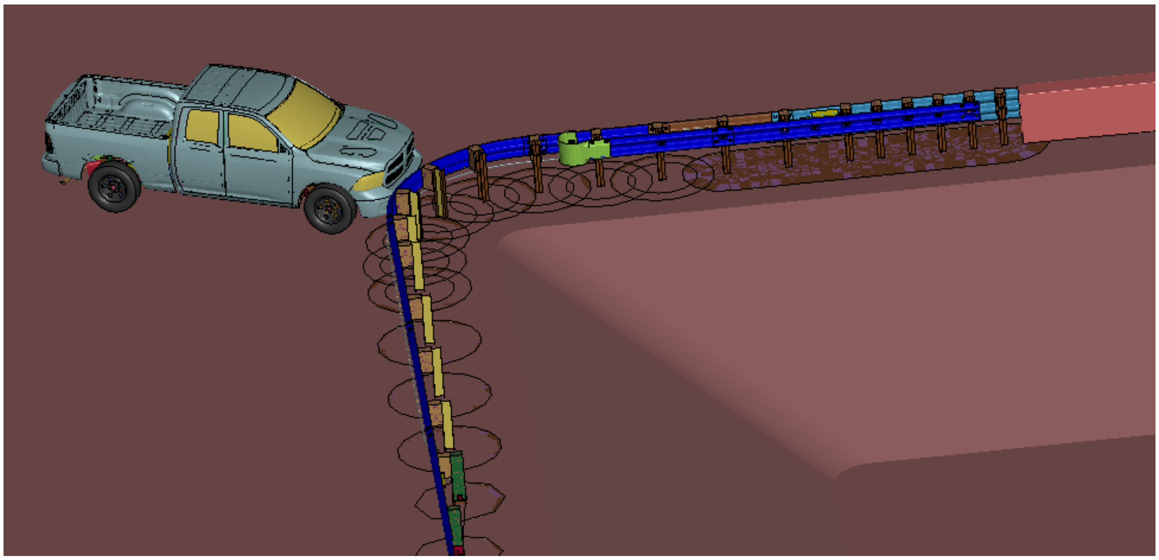

MASH TL-3 ENHANCEMENT OF THE SHORT RADIUS GUARDRAIL SYSTEM (SRGS) IN FRONT OF 2:1 SLOPE – DESIGN MODIFICATION

Sponsored by

WASHINGTON STATE DEPARTMENT OF TRANSPORTATION (WSDOT)

TEXAS A&M TRANSPORTATION INSTITUTE
Roadside Safety & Physical Security
Texas A&M University System
RELLIS Campus
Building 7091
1254 Avenue A
Bryan, TX 77807

Technical Report Documentation Page

1. Report No.	2. Government Accession No.	3. Recipient's Catalog No.
4. Title and Subtitle MASH TL-3 ENHANCEMENT OF THE SHORT RADIUS GUARDRAIL SYSTEM (SRGS) IN FRONT OF 2:1 SLOPE – DESIGN MODIFICATION		5. Report Date August 2026 6. Performing Organization Code
7. Author(s) Sun Hee Park, Hongseok Kim, Akram Abu-Odeh, and Nauman M. Sheikh		8. Performing Organization Report No. TRNo. 620841
9. Performing Organization Name and Address Texas A&M Transportation Institute Proving Ground 3135 TAMU College Station, Texas 77843-3135		10. Work Unit No. (TRAIS) 11. Contract or Grant No. Contract T1969-AN
12. Sponsoring Agency Name and Address Washington State Department of Transportation Research Office MS 47372 Transportation Building Olympia, WA 98504-7372		13. Type of Report and Period Covered Technical Report: First Test Month Year - August 2026 14. Sponsoring Agency Code
15. Supplementary Notes Name of Contracting Representative: Tim Moeckel, WSDOT		

16. Abstract

States face challenges providing crashworthy barrier systems at intersections where side roads or driveways are close to structures on major roads. The short radius guardrail system (SRGS) developed under NCHRP Project 15-53 is an effective barrier option but is currently only MASH Test Level 3 (TL-3) compliant on flat ground. The SRGS was tested at an impact speed of 50 mph when placed in front of a 2:1 slope and is considered MASH Test Level 2 (TL-2) compliant in this configuration. There is potential to improve the SRGS for broader use, and more cost-effective construction through design modifications. A survey of the Roadside Safety Pooled Fund member states showed the greatest interest in developing a MASH TL-3 compliant design for the SRGS when placed in front of a 2:1 slope by making modifications to the system developed under NCHRP Project 15-53.

This project investigates several potential design modifications of the SRGS when placed in front of a 2:1 slope that is compliant with MASH TL-3. A finite element model of the SRGS system was validated from previous tests, and modified SRGS designs were evaluated through impact simulations under TL-3 conditions. Details of modified designs are described, and recommendations for full-scale testing of the modified designs are presented herein.

17. Key Words	18. Distribution Statement
Short Radius Guardrail System, Guardrail, LS-DYNA, FE simulation, Impact Simulation, MASH,	No restrictions. This document is available to the public through NTIS: National Technical Information Service Alexandria, Virginia 22312 http://www.ntis.gov

19. Security Classification. (of this report)	20. Security Classification. (of this page)	21. No. of Pages	22. Price
Unclassified	Unclassified	41	

Form DOT F 1700.7 (8-72) Reproduction of completed page authorized.

MASH TL-3 ENHANCEMENT OF THE SHORT RADIUS GUARDRAIL SYSTEM (SRGS) IN FRONT OF 2:1 SLOPE – DESIGN MODIFICATION

by
Sun Hee Park, Ph.D.
Associate Transportation Researcher
Texas A&M Transportation Institute

Hongseok Kim
Graduate Student Researcher
Texas A&M Transportation Institute

Akram Y. Abu-Odeh, Ph.D.
Research Scientist (Retired)
Texas A&M Transportation Institute

and

Nauman M. Sheikh, P.E.
Senior Research Engineer
Texas A&M Transportation Institute

Report 620841
Contract No.: T1969-AN

Sponsored by the

Washington State Department of Transportation

August 2026

TEXAS A&M TRANSPORTATION INSTITUTE
College Station, Texas 77843-3135

DISCLAIMER

The contents of this report reflect the views of the authors, who are solely responsible for the facts and accuracy of the data and the opinions, findings, and conclusions presented herein. The contents do not necessarily reflect the official views or policies of the Roadside Safety Pooled Fund, The Texas A&M University System, or the Texas A&M Transportation Institute (TTI). This report does not constitute a standard, specification, or regulation. In addition, the above listed agencies/companies assume no liability for its contents or use thereof. The names of specific products or manufacturers listed herein do not imply endorsement of those products or manufacturers.

ACKNOWLEDGEMENTS

This research project was performed under a pooled fund program between the following States and Agencies. The authors acknowledge and appreciate their guidance and assistance.

Roadside Safety Research Pooled Fund Committee
Revised July 2026

ALABAMA

Wade Henry, P.E.
Assistant State Design Engineer
Design Bureau, Final Design Division
Alabama Dept. of Transportation
1409 Coliseum Boulevard, T-205
Montgomery, AL 36110
(334) 242-6464
henryw@dot.state.al.us

Stanley (Stan) C. Biddick, P.E.
State Design Engineer
Alabama Dept. of Transportation
1409 Coliseum Boulevard, T-205
Montgomery, AL 36110
(334) 242-6488
biddicks@dot.state.al.us

ALASKA

Micheal Hills
Internal Consultant
Alaska Department of Transportation &
Public Facilities
3132 Channel Drive
Juneau, AK 99801
(907) 465-2645
micheal.hills@alaska.gov

Brandon Irvine
Preconstruction Standards Engineer
Alaska Department of Transportation &
Public Facilities
2301 Peger Road, Fairbanks, AK 99709
(907) 451-5388
brandon.irvine@alaska.gov

CALIFORNIA

Vue Her, P.E.
Chief, Crash Test Operations
California Department of Transportation
Division of Research, Innovation and
System Information
Roadside Safety Research Group
5900 Folsom Blvd, MS-5
Sacramento, CA 95819
(916) 227-5828
vue.her@dot.ca.gov

Christopher Caldwell, P.E.
Transportation Engineer
California Department of Transportation
Division of Research, Innovation and
System Information
Roadside Safety Research Group
5900 Folsom Blvd, MS-5
Sacramento, CA 95819
(916) 591-2877
christopher.caldwell@dot.ca.gov

COLORADO

David Kosmiski, P.E.
Miscellaneous (M) Standards Engineer
Colorado Dept. of Transportation (CDOT)
2829 W Howard Pl (3rd fl southwest),
Denver, CO 80204
david.kosmiski@state.co.us

Andy Pott, P.E.
Bridge/Structure Senior Design and
Construction Engineer
Colorado Dept. of Transportation (CDOT)
2829 W Howard Pl (3rd fl southwest),
Denver, CO 80204
(720) 454-4045

andrew.pott@state.co.us

Bill Cornelius, P.E.
Roadway Standards and specifications Unit Manager/Engineer
Colorado Dept. of Transportation (CDOT)
2829 W Howard Pl (3rd fl southwest),
Denver, CO 80204
bill.cornelius@state.co.us

Amin Fakhimalizad
Assistant Miscellaneous (M) Standards Engineer
Colorado Dept. of Transportation (CDOT)
2829 W Howard Pl (3rd fl southwest),
amin.fakhimalizad@state.co.us

Man (Steven) Yip
Bridge/Structure Design and construction Support Engineer
Colorado Dept. of Transportation (CDOT)
2829 W Howard Pl (3rd fl northeast),
Denver, CO 80204
(303) 269-1262
man.yip@state.co.us

CONNECTICUT

Todd Ingarra
Transportation Engineer 3
Engineering Services/Facilities & Transit
Connecticut Department of Transportation
(860)594-3292
todd.ingarra@ct.gov

DELAWARE

Cassidy Blowers
Construction Resource Engineer
Construction Section
Delaware DOT
(302) 760-2336
Cassidy.Blowers@delaware.gov

James Osborne
Traffic Safety Programs Manager
Traffic Operations
Delaware DOT
(302) 659-4651
James.Osborne@delaware.gov

FLORIDA

Richard Stepp
State Roadway Design Engineer
Florida Department of Transportation
Roadway Design Office
605 Suwannee Street, MS-32
Tallahassee, FL 32399-0450
(850) 414-4313
Richard.Stepp@dot.state.fl.us

IDAHO

Marc Danley, P.E.
Technical Engineer
(208) 334-8558
Marc.danley@itd.idaho.gov

Kevin Sablan
Design/Traffic Engineer
Idaho Transportation Department
(208) 334-8558
Kevin.sablan@itd.idaho.gov

ILLINOIS

Martha A. Brown, P.E.
Safety Policy & Initiatives Engineer
Bureau of Safety Programs and Engineering
Illinois Department of Transportation
2300 Dirksen Parkway, Room 005
Springfield, IL 62764
(217) 785-3034
Martha.A.Brown@illinois.gov

Edgar A. Galofre, MSCE, P.E.
Safety Design Engineer
Bureau of Safety Programs and Engineering
Illinois Department of Transportation
2300 S. Dirksen Parkway, Room 007
Springfield, IL 62764
(217) 558-9089
Edgar.Galofre@illinois.gov

Kelli Erickson
Safety Design Evaluation Engineer
Bureau of Safety Programs and Engineering
Illinois Department of Transportation
2300 S. Dirksen Parkway, Room 007
Springfield, IL 62764
(217) 557-2563
Kelli.Erickson@Illinois.gov

IOWA

Daniel Harness
Design Bureau – Methods Section
Iowa Department of Transportation
Daniel.Harness@iowadot.us

Chris Poole
State Traffic Engineer
Traffic and Safety Bureau
Iowa Department of Transportation
Chris.Poole@iowadot.us

LOUISIANA

Ryan Owens
Bridge & Structural Design Section
Louisiana Department of Transportation
ryan.owens@la.gov

MARYLAND

Vivian Berra Figuereo
VBerraFiguereo@mdot.maryland.gov

Philip Brentlinger
Maryland State Highway Administration
pbrentlinger@mdot.maryland.gov

MASSACHUSETTS

James Danila
State Traffic Engineer
Massachusetts Depart. of Transportation
10 Park Plaza
Boston, MA 02116
James.danila@state.ma.us

Alex Bardow
State Bridge Engineer
Massachusetts Depart. of Transportation
10 Park Plaza
Boston, MA 02116
(857) 368-9430
Alexander.Bardow@state.ma.us

MICHIGAN

Carlos Torres, P.E.
Roadside Safety Engineer
Geometric Design Unit, Design Division
Michigan Depart. of Transportation
P.O. Box 30050
Lansing, MI 48909
(517) 335-2852
TorresC@michigan.gov

MINNESOTA

Khamsai Yang
State Design Standards Engineer
Office of Project Management and
Technical Support
Minnesota Department of Transportation
395 John Ireland Blvd, MS 551155
(612) 322-5601
Khamsai.Yang@state.mn.us

Brian Tang
Assistant Design Standards Engineer
Office of Project Management and
Technical Support
Minnesota Department of Transportation
395 John Ireland Blvd, MS 551155
(651) 633-4684
brian.tang@state.mn.us

MISSOURI

Gidget Koestner
Policy & Innovations Engineer
Central Office- Design
Missouri Department of Transportation
(573) 751-6905
gidget.koestner@modot.mo.gov

Kirby Woods
Roadside Design Engineer
Missouri Department of Transportation
(573) 472-5333
kirby.woodsjr@modot.mo.gov

NEW MEXICO

Brad Julian
New Mexico Department of Transportation
Traffic Technical Support Engineer
(505) 469-1405
Brad.Julian@dot.nm.gov

NEVADA

David Fox, P.E.
Specifications Engineer
Roadway Design Division
Nevada Dept. of Transportation
1263 S. Stewart St.
Carson City, NV 89712
(775) 888-7053
DWFox@dot.nv.gov

Tim Rudnick
Standards and Manuals Supervisor
Roadway Design Division
Nevada Dept. of Transportation
1263 S. Stewart St.
Carson City, NV 89712
(775) 888-7598
TRudnick@dot.nv.gov

OHIO

Don P. Fisher, P.E.
Ohio Depart. of Transportation
1980 West Broad Street
Mail Stop 1230
Columbus, OH 43223
(614) 387-2614
Don.fisher@dot.ohio.gov

Andrew Holloway, P.E.
(614) 387-4020
Andrew.Holloway@dot.ohio.gov

OREGON

Christopher Henson
Senior Roadwas/Roadside Design Engineer
Oregon Depart. of Transportation
Technical Service Branch
(971) 208-4989
Christopher.S.Henson@odot.state.or.us

PENNSYLVANIA

James A. Borino, Jr., P.E.
Chief, Standards and Criteria Unit
Highway Design and Technology Division
Pennsylvania DOT
(717) 612-4791
jborino@pa.gov

Evan Pursel
Senior Civil Engineer
Highway Design and Technology Division
Pennsylvania DOT
(717) 705-8535
epursel@pa.gov

Nina Ertel
Project Development Engineer
Highway Design and Technology Division
Pennsylvania DOT
(717) 425-7679
nertel@pa.gov

TENNESSEE

Tsehay Dessalgn
Statewide Transportation Engineer
Engineering Division – Production Support
Tennessee Dept. of Transportation
(615) 532-2614
Tsehay.Dessalgn@tn.gov

Laura Chandler
Engineering Production Support Manager
Engineering Division
Tennessee Dept. of Transportation
(615) 253-4769
Laura.Chandler@tn.gov

Wesely Apple
Design Quality – Team Lead
(615) 770-6815
wesley.apple@tn.gov

TEXAS

Chris Lindsey
Transportation Engineer
Design Division
Texas Department of Transportation
125 East 11th Street
Austin, TX 78701-2483
(512) 416-2750
Christopher.Lindsey@txdot.gov

Taya Retterer
TxDOT Bridge Standards Engineer
Bridge Division
Texas Department of Transportation
(512) 993-0330
Taya.Retterer@txdot.gov

Wade Odell
Research Project Manager
Research & Technology Implementation Division
Texas Department of Transportation
(512) 416-4737
wade.odell@txdot.gov

UTAH

Clint McCleery
Barrier and Attenuation Specialist
Traffic and Safety Operations
Utah Department of Transportation
4501 South 2700 West
Taylorsville, UT 84129
(801)712-8685
cmccleery@utah.gov

WASHINGTON

Tim Moeckel
Roadside Safety Engineer
Washington State Department of Transportation
Development Division
(360) 704-6377
moecket@wsdot.wa.gov

Mustafa Mohamedali
Research Manager/Engineering
Transportation Safety & System Analysis
Research & Library Services
(360) 704-6307
mohamem@wsdot.wa.gov

Kevin Burch
Policy Support Engineer
Washington State Department of Transportation
Development Division
(360) 705-7952
burchk@wsdot.wa.gov

WEST VIRGINIA

Ted Whitmore
Traffic Services Engineer
Traffic Engineering
WV Division of Highways
(304)414-7373
Ted.J.Whitmore@wv.gov

WISCONSIN

Erik Emerson, P.E.
Standards Development Engineer – Roadside Design
Wisconsin Department of Transportation
Bureau of Project Development
Room S424.03
4822 Madison Yards Way, Madison 53705
(608) 266-2842
Erik.Emerson@wi.gov

CANADA – ONTARIO

Kenneth Shannon, P. Eng.
Lead Engineer, Highway Design
Ontario Ministry of Transportation
301 St. Paul Street
St. Catharines, ON L2R 7R4
CANADA
(289) 783-4348
Kenneth.Shannon@ontario.ca

FEDERAL HIGHWAY ADMINISTRATION (FHWA)
Website: safety.fhwa.dot.gov

Eduardo Arispe
Research Highway Safety Specialist
U.S. Department of Transportation
Federal Highway Administration
Turner-Fairbank Highway Research Center
6300 Georgetown Pike
McLean, VA 22101
(202) 493-3291
Eduardo.arispe@dot.gov

Paul LaFleur, P.E.
Safety Design Team - Roadway Departure
Program Manager
FHWA Office of Safety
U.S. Department of Transportation
(515) 233-7308
paul.lafleur@dot.gov

TEXAS A&M TRANSPORTATION INSTITUTE (TTI)
Website: tti.tamu.edu
www.roadsidepooledfund.org

D. Lance Bullard, Jr., P.E.
Senior Research Engineer
Roadside Safety & Physical Security Div.
Texas A&M Transportation Institute
3135 TAMU
College Station, TX 77843-3135
(979) 317-2855
L-Bullard@tti.tamu.edu

Roger P. Bligh, Ph.D., P.E.
Senior Research Engineer
Roadside Safety and Physical Security
Division
(979) 317-2703
R-Bligh@tti.tamu.edu

Nauman Sheikh, P.E.
Senior Research Engineer
Roadside Safety and Physical Security
Texas A&M Transportation Institute
(979) 317-2703
n-sheikh@tti.tamu.edu

Ariel Sheil
Research Assistant
Roadside Safety and Physical Security
Texas A&M Transportation Institute
(979) 317-2250
A-Sheil@tti.tamu.edu

TABLE OF CONTENTS

LIST OF FIGURES

Page

LIST OF TABLES

Page

SI* (MODERN METRIC) CONVERSION FACTORS				
APPROXIMATE CONVERSIONS TO SI UNITS				
Symbol	**When You Know**	**Multiply By**	**To Find**	**Symbol**
		LENGTH		
in	inches	25.4	millimeters	mm
ft	feet	0.305	meters	m
yd	yards	0.914	meters	m
mi	miles	1.61	kilometers	km
		AREA		
in^2	square inches	645.2	square millimeters	mm^2
ft^2	square feet	0.093	square meters	m^2
yd^2	square yards	0.836	square meters	m^2
ac	acres	0.405	hectares	ha
mi^2	square miles	2.59	square kilometers	km^2
		VOLUME		
fl oz	fluid ounces	29.57	milliliters	mL
gal	gallons	3.785	liters	L
ft^3	cubic feet	0.028	cubic meters	m^3
yd^3	cubic yards	0.765	cubic meters	m^3
		NOTE: volumes greater than 1000L shall be shown in m^3		
		MASS		
oz	ounces	28.35	grams	g
lb	pounds	0.454	kilograms	kg
T	short tons (2000 lb)	0.907	megagrams (or metric ton")	Mg (or "t")
		TEMPERATURE (exact degrees)		
°F	Fahrenheit	5(F-32)/9 or (F-32)/1.8	Celsius	°C
		FORCE and PRESSURE or STRESS		
lbf	poundforce	4.45	newtons	N
lbf/in^2	poundforce per square inch	6.89	kilopascals	kPa
APPROXIMATE CONVERSIONS FROM SI UNITS				
Symbol	**When You Know**	**Multiply By**	**To Find**	**Symbol**
		LENGTH		
mm	millimeters	0.039	inches	in
m	meters	3.28	feet	ft
m	meters	1.09	yards	yd
km	kilometers	0.621	miles	mi
		AREA		
mm^2	square millimeters	0.0016	square inches	in^2
m^2	square meters	10.764	square feet	ft^2
m^2	square meters	1.195	square yards	yd^2
ha	hectares	2.47	acres	ac
km^2	Square kilometers	0.386	square miles	mi^2
		VOLUME		
mL	milliliters	0.034	fluid ounces	oz
L	liters	0.264	gallons	gal
m^3	cubic meters	35.314	cubic feet	ft^3
m^3	cubic meters	1.307	cubic yards	yd^3
		MASS		
g	grams	0.035	ounces	oz
kg	kilograms	2.202	pounds	lb
Mg (or "t")	megagrams (or "metric ton")	1.103	short tons (2000lb)	T
		TEMPERATURE (exact degrees)		
°C	Celsius	1.8C+32	Fahrenheit	°F
		FORCE and PRESSURE or STRESS		
N	newtons	0.225	poundforce	lbf
kPa	kilopascals	0.145	poundforce per square inch	lb/in^2

*SI is the symbol for the International System of Units

CHAPTER 1. INTRODUCTION

1.1. BACKGROUND

States have a long-standing problem when trying to provide crashworthy barrier systems at intersection locations where a side road or driveway intersects near a bridge or structure end on a major road. Often, the proximity of the intersecting side road or driveway does not allow enough room to properly install a longitudinal barrier system that can adequately shield mainline traffic from the bridge or structure end and/or the slope immediately adjacent to it. Due to this issue, a project funded by the National Cooperative Highway Research Program (NCHRP) led to the development of a Manual for Assessing Safety Hardware (MASH) [1] compliant Short-Radius Guardrail System (SRGS) by Powers et al. documented in NCHRP Project 15-53 [2, 3]. This system provides an effective barrier option at intersection locations for state transportation agencies. The system developed under NCHRP Project 15-53 is shown in Figure 1.1.

Currently, the SRGS is MASH Test Level 3 (TL-3) compliant on flat ground and MASH TL-2 compliant when placed in front of a 2:1 or flatter slope (tested at 50 mph). Based on simulations performed during NCHRP Project 15-53 [2, 3], the SRGS in front of a 2:1 slope indicated a higher possibility of failing tests with an impact speed of 56 mph (90 km/hr) or higher (MASH TL-3 tests) due to vehicle stability concerns shown by significant roll and pitch angles of the vehicle.

There are opportunities to explore and improve the SRGS design through design modifications to make it more effective, accessible for use at a higher number of locations, and simpler/more cost-effective to construct. A preliminary survey was given to the Roadside Safety Pooled Fund member states ranking their interest in potential SRGS modifications/enhancements. The survey showed that the greatest interest was to modify the SRGS as needed to successfully meet MASH TL-3 crash testing criteria when placed in front of a 2:1 slope.

Figure 1.1. The NCHRP 15-53 SRGS Design Overview [2, 3]

1.2. OBJECTIVE

The objective of this study is to investigate potential modifications/enhancements to the SRGS developed under NCHRP Project 15-53 [2, 3] in order to achieve MASH TL-3 compliance crash testing requirements when placed in front of a 2:1 embankment slope. As an extension of the original NCHRP Project 15-53, this study encompasses both researching advancements beyond what was accomplished in the original project scope and cross-validation with prior findings from NCHRP Project 15-53 to ensure simulation accuracy to the maximum extent feasible.

CHAPTER 2.
LITERATURE REVIEW

2.1. INTRODUCTION

This chapter reviews past relevant studies of the MASH complaint short radius guardrail (SRGS) and similar systems. SRGS systems are intended to be used at intersection locations where geometric restrictions exist which limit available longitudinal barrier installation length. Such conditions commonly occur near bridge rail ends when placed in proximity to roadway intersections, driveways, and/or steep embankments. At these locations, conventional tangent or flared barrier runs require substantial run-out/length of need distances that are often impractical or infeasible to install. As a result, alternative compact radius guardrail systems capable of meeting high-speed crashworthiness requirements have been actively investigated through the years.

Older research and development of early short-radius guardrail systems prior to the MASH era generally failed to meet high-speed TL-3 criteria due to vehicle instability, rail rupture, localized pocketing, and/or insufficient energy dissipation. More recent MASH era research, described in Sections 2.2 through 2.4 below, introduced refined design concepts which included: modified rail geometries, enhanced post configurations, improved anchorage systems, and integrated mass-dissipation mechanisms. These innovations were intended to control vehicle redirection, mitigate underride, limit occupant risk factors, and improve overall vehicle stability under TL-3 conditions.

This literature review summarizes MASH era research related to the SRGS. It summarizes the key challenges encountered in prior studies, the principal design features and concepts that were crash tested, and the performance outcomes of each research project.

2.2. NCHRP PROJECT 15-53 – ROADSIDE BARRIER DESIGNS NEAR BRIDGE RAIL ENDS WITH RESTRICTED RIGHTS-OF-WAY - A GUIDE [2, 3] AND TEST REPORT [3]

The purpose of NCHRP Project 15-53 [2, 3] was to develop a short-radius guardrail system (SRGS) design that complied with MASH TL-3. Figure 2.1 shows details of the SRGS barrier system developed under the project. The system successfully met MASH TL-3 evaluation criteria on flat ground, and met MASH TL-2 evaluation criteria when placed in front of a 2:1 slope. The design process of the SRGS relied on extensive use of finite-element (FE) modeling to evaluate various system configuration changes and then culminated with full-scale crash testing.

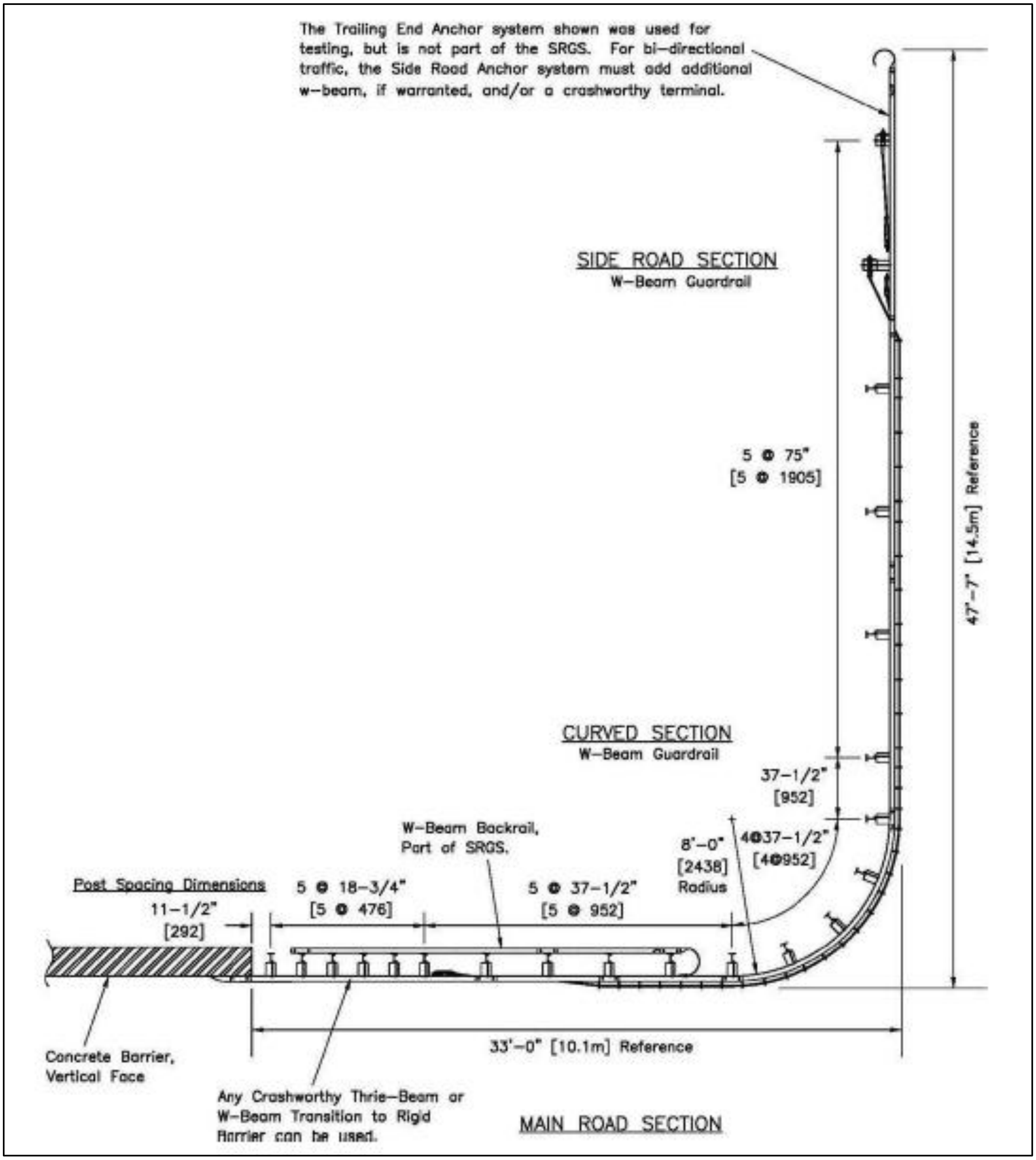

Figure 2.1. Details of SRGS Developed Under NCHRP 15-53 [2, 3]

2.2.2. Iterative Simulation-Based Design Development

Five design concepts based on the Midwest Guardrail System (MGS) were iteratively assessed through simulation as part of the SRGS refinement process. The details of each iteration are summarized in Table 2.1. Of the five design concepts, this section discusses the three concepts most directly relevant to this study.

The first concept, addressed through simulation Iterations 2 and 3, focused on the mitigation of passenger vehicle underride. Simulations replicating the impact conditions of MASH Test 3-32 (passenger car impact into the curved nose section at a 15-degree angle) revealed significant underride beneath the 31-in. W-beam rail. To mitigate this behavior, two continuous steel cables were incorporated: one cable positioned within the W-beam valley and a second cable located approximately 5 inches below the W-beam rail. Both cables were anchored at the terminal ends which collectively restrained rail uplift and substantially reduced the risk of passenger vehicle underride upon impact.

The second concept, addressed through Iteration 4, focused on the meeting the need for increased structural stiffness and limiting the deflection of the SRGS. Simulations of previous iterations had identified localized pocketing and excessive deformation in the curved radius segment during Test 3-31 (pickup truck impacting the curved section at a 0-degree angle parallel to the main road). To address these two issues, Iteration 4 introduced additional posts within the curved radius area to stiffen the section and lowered the cable position below the W-beam rail to enhance barrier engagement with smaller vehicles. These modifications successfully stiffened the curved section of the system, eliminated indications of pocketing, and improved overall system performance in subsequent Test 3-31 simulations.

The third concept, addressed through Iteration 5, further refined the SRGS system design to optimize standard hardware components. This concept introduced the use of standard 6-ft long steel posts (replacing wood posts) and 8-in. deep blockouts, while also adding a second steel cable along the center valley of the W-beam rail. These modifications were assessed through computer simulations of MASH Test 3-35 conditions (pickup truck impacting the transition section on the main road with an impact speed of 62 mph (100 km/hr) and a 25-degree impact angle). The results confirmed that Iteration 5 successfully redirected the vehicle under oblique impact conditions and satisfied MASH evaluation criteria.

Table 2.1. Summary of Simulation Iterations of MGS-based Concept

Simulation Iteration No.	System Design Concept	MASH Test 3-31*	MASH Test 3-32	MASH Test 3-33	MASH Test 3-35
1	- MGS rail with 12 in. block - PennDOT Transition, W-beam and rubrail	Did not meet	Met	Did not meet	Did not meet
2	- MGS rail with 12 in. block - Missouri Transition, 10-gauge thrie-beam - Cable anchor at LON point	Did not meet	Did not meet	Met	Did not meet
3	- Use 10-gauge for entire system - Change to wood post - Add a post downstream from radius - Attach cable to a separate ground anchor in the radius - Run a cable beneath W-beam	Did not meet	Did not meet	Met	Met
4	- Add posts in curved section - Lower cable placed beneath W-beam	Met	Marginal	Met	Met
5	- Replace wood post with 6 ft long steel post - Use 8 in. blockouts - Add cable in center valley of rail	Met	Met	Met	Met

**Test parameters are listed in Table 2.2 test matrix*

Table 2.2. MASH Test Matrix Performed under NCHRP Project 15-53

Test No.	Vehicle	Impact Speed	Impact Angle	Impact Location
3-31	Pickup Truck	62 mph	0 degree	Curved section center
3-32	Passenger Car	62 mph	15 degrees	Curved section center
3-33	Pickup Truck	62 mph	15 degrees	Curved section center
3-35	Pickup Truck	62 mph	25 degrees	Transition on main road

The performance of the fifth conceptual design was further evaluated to investigate the crashworthiness of the SRGS placed in front of various slopes ranging from 2:1 to 6:1 with different flat bench section widths behind the post under MASH TL-3 conditions. The simulation results are summarized in Table 2.3. While the SRGS passed all simulation evaluations with the 1100C passenger car, its performance with the 2270P pickup truck was mixed due to being highly sensitive to slope grade. The only configuration indicating it was likely to pass MASH TL-3 tests for both vehicles was the SRGS in front of the 6:1 slope. The predicted performance with the pickup truck indicated "Marginal" or "Fail" ratings on all slopes steeper than 6:1.

Table 2.3. Summary of Simulations for SRGS without Backrail in front of Various Slopes Performed under NCHRP Project 15-53 [2, 3]

		Passenger Car 2ft Bench	Passenger Car 3ft Bench	Passenger Car 4ft Bench	Pickup Truck 2ft Bench	Pickup Truck 3ft Bench	Pickup Truck 4ft Bench
Back Slope	**6H:1V**	Pass	Pass	Pass	Pass	Pass	Pass
	4H:1V	Pass	Pass	Pass	Fail	Marginal	Marginal
	3H:1V	Pass	Pass	Pass	Fail	Fail	Marginal
	2H:1V	Pass	Pass	Pass	Fail	Fail	Fail

2.2.3. Full-Scale Crash Testing and Targeted Modifications

The initial SRGS full-scale MASH Tests on flat terrain included Tests 3-31, 3-32, 3-33, and 3-35 (see Table 2.2). During testing, initial MASH Test 3-33 (FOIL Test 19012:2270P pickup truck impacting the center post of the curved section at 62.5 mph and 15 degrees) failed due to an excessive vehicle roll angle causing the pickup truck to roll over on its side. In response to the failed test, the project team modified the SRGS by attaching an additional 18 ft 9 in. length of 10-gauge W-beam to the back side of the posts of the thrie-beam transition section with no blockouts. The subsequent MASH Test 3-33 (FOIL Test 20004) was successfully contained and redirected the pickup truck in a stable manner without excessive roll angle and rollover. The other MASH tests of the SRGS on flat terrain all passed.

Although the SRGS met the required MASH TL-3 criteria on flat terrain, additional simulations and crash tests were needed to assess its performance under a broader range of field conditions. This included configurations of the SRGS when placed in front of steep slopes, and providing guidance for implementation with different system radii than the crash tested 8-foot radius. Results of simulations for SRGS installations in front of steep slopes indicated unacceptable performance when impacted at high-speeds (TL-3). The project team performed reduced speed simulations of MASH Test 3-33 with the SRGS in front of a 2:1 slope. The 50 mph (80 km/h) impact speed simulation indicated the SRGS would successfully contain the test vehicle. Based off the simulation results, the project team opted to conduct Test 3-33 (FOIL TEST 20012) of the SRGS in front of a 2:1 slope with a pickup truck impacting the nose of the system at 50 mph (80 km/h). In these tests, the cable elements effectively prevented the vehicle from penetrating the system and descending the slope when the 10-gauge W-beam rail ruptured. Next, results of simulations with larger curve radii (16-ft. and 24-ft. radii) indicated that the SRGS will likely maintain satisfactory crashworthy performance. The simulations indicated only minor increases in vehicle roll motions that remained within acceptable safety limits for the larger system radii. Finally, guidance for alternative installation configurations was developed for symmetric SRGS installations lacking an adjacent bridge rail to connect to. Also, guidance for connecting the SRGS to other MASH-compliant transitions, W-beam, or thrie-beam systems was developed, enhancing its availability for use at varied site conditions.

NCHRP Project 15-53 addressed a longstanding safety challenge at bridge ends experiencing constrained geometry where conventional tangent or flared guardrail runs (or end treatments) are infeasible due to intersecting driveways/roadways, steep slopes, or other urban restrictions. The resulting SRGS provides a compact, crashworthy barrier alternative capable of achieving MASH TL-3 redirection with acceptable occupant risk factors while significantly reducing required mainline tangent installation length.

Please note that the SRGS was MASH TL-3 compliant only when placed on flat ground. The performance of the SRGS when placed in front of a 2:1 slope (or flatter) was evaluated at a lower speed of 50 mph (80 km/h). As a result, the SRGS is only considered MASH TL-2 compliant when placed in front of a 2:1 slope. Therefore, further design improvement and evaluation under high-speed MASH TL-3 conditions are necessary for this particular SRGS system.

2.3. MASH CRASH TESTING AND SIMULATION EVALUATION OF VARIATIONS OF THE TXDOT SHORT-SPAN SHORT-RADIUS GUARDRAIL SYSTEM [4, 5]

The purpose of research for TTI/TXDOT Test Report 9-1002-15-9 was to develop and evaluate a crashworthy short-span short-radius guardrail system that satisfied MASH TL-3 criteria in highly constrained roadside environments, particularly adjacent to bridge rail termini. Historically, past short-radius system configurations were unable to meet the high-speed TL-3 performance requirements of NCHRP Reports 230 and 350 and by extension the subsequently more demanding MASH testing criteria which introduced larger test vehicles and expanded impact conditions.

Under flat-ground conditions, the Texas Department of Transportation (TxDOT) SRGS achieved full MASH TL-3 compliance through a series of full-scale tests (MASH Tests 3-31, 3-32, 3-33, and 3-35) which collectively demonstrated stable containment, acceptable redirection, and vehicle stability (no rollover) for both the pickup truck and the passenger cars under head-on and oblique impacts. Figure 2.2 shows different views of the TXDOT SRGS installation from the MASH TL-3 tests. The crashworthy configuration employed a 31-inch-tall thrie-beam rail with an 8 ft-4½ in inside radius, a tension cable extending across the nose section to sustain longitudinal tension during redirection, and 4 strategically placed frangible sand barrels that assisted with energy dissipation and control of stopping distance while maintaining occupant risk factors measure within MASH limits.

Figure 2.2. TXDOT Short-Radius Guardrail MASH TL-3 setup [5]

Figure 2.3 illustrates the three primary nose-impact tests: Tests 3-31, 3-32, and 3-33. Test 3-31 assesses the head-on impact of the pickup truck with the system, where the vehicle's centerline is aligned directly with the traffic face of the rigid bridge parapet. Test 3-32 evaluates a passenger car impacting the center post of the curved section at 15 degrees. Test 3-33 evaluates the pickup impacting the center post of the curved section at 15 degrees.

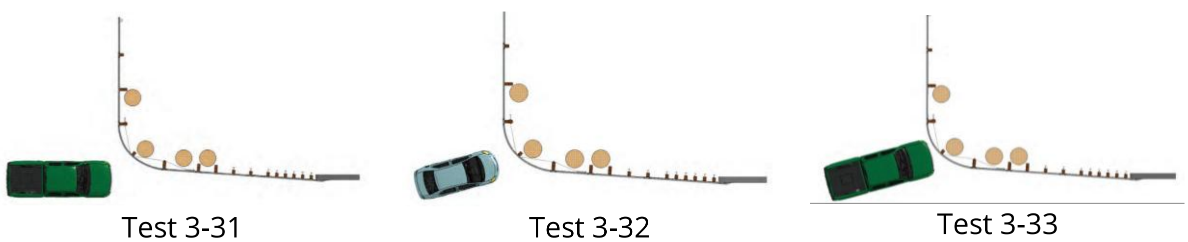

Figure 2.3. Target Critical Impact Points(CIP) for MASH Test 3-31, 32, 33 on the TxDOT SRGS treatment [5]

To better represent a wider range of field conditions, the TXDOT SRGS was subsequently evaluated in front of a 3:1 slope and crash tested with a modified impact angle of 25 degrees into the nose of the system for both the 2270P pickup truck (modified Test 3-33) and the 1100C passenger car (modified Test 3-32). The impact angle was increased from 15- to-25 degrees because the SRGS functions not only as a bridge rail end terminal but also as a longitudinal barrier. The 25-degree angle is the designated impact angle for a longitudinal barrier as described in MASH [1]. It was also selected based on the simulation analysis indicating that the steeper angle represented a more critical impact condition for the passenger car when compared to the 15-degree angle. Although simulations of the pickup truck showed no significant sensitivity to the change in angle, the 25-degree impact was utilized for both tests to ensure the system was evaluated against the most critical conditions.

In Tests 3-32 and 3-33, the impact angle of 25 degrees was measured from the face of the bridge parapet, and the critical impact point (CIP) corresponds to the face of the rail at the center post near the nose of the radius. In both tests, the SRGS successfully contained the vehicles on the field side, maintained vehicle stability with moderate roll and pitch angles, and satisfied all relevant MASH evaluation criteria. While Test 3-31 was a critical requirement for initial certification on flat terrain, it was deemed non-critical for evaluations involving steep slopes and was subsequently omitted from those testing matrices. Researchers determined that the performance of the redirection-focused Test 3-31 would not be significantly affected by the slope behind the SRGS because the impact is centered on the rigid bridge rail transition, where the system's structural stiffness, rather than the terminal region's capture behavior, governs the outcome.

Next, follow-up TXDOT/TTI research project No. 604661 was conducted which performed complementary simulation studies examining different TXDOT SRGS design variations. The study focused on hybrid configurations that combined TL-3 primary-road elements, such as a 31-inch tall Thrie-beam guardrail, with TL-2 secondary road components like W-beam rail joined by an asymmetric connector. To enhance vehicle stability, the system utilized an increased 16-foot inside radius for the curved section, which featured 11-inch long slots to control rail deformation during impact. In addition, six 700-lb sand drums were strategically placed on the field side to provide required energy dissipation. The simulations indicated acceptable pickup truck performance for 25-degree impacts. The steeper 25-degree angle was chosen because it was identified as more critical for passenger car stability. The 25-degree simulations indicated potential exceedances in passenger car occupant impact velocity. These findings prompted recommendations for full-scale crash testing to validate the predictive results.

2.4. MASH TESTING OF THE THRIE-BEAM BULLNOSE SYSTEM PHASE 1 [6] & PHASE 2 [7]

Figure 2.4 shows MwRSF thrie-beam bullnose system. The MASH evaluation of the system proceeded in two phases starting with an initial design concept utilizing Universal Breakaway Steel Posts (UBSPs). In Phase 1 (MwRSF Research Report No. TRP-03-389-20), the initial design successfully conducted three critical tests (3-32, 3-34 and 3-35) aimed at evaluating severe impact scenarios, particularly where the bullnose system transitions between capturing and redirecting an impacting vehicle. Test MSPBN-1 was tested under MASH 3-35 criteria (2270P pickup truck impacting the bullnose system's Critical Impact Point (CIP) at an impact angle of 25 degrees) testing the system's transition area changing from vehicle capture to vehicle redirection. Test MSPBN-2 was conducted under MASH 3-34 criteria (1100C passenger car impacting the bullnose system's CIP at 15 degrees) testing the system's transition area changing from vehicle capture to vehicle redirection with the lighter vehicle. Test MSPBN-3 was conducted under MASH 3-32 criteria (1100C passenger car impacting the bullnose center at 15 degrees) to evaluate oblique impacts on the end of the system. Phase 1 crash testing demonstrated that the bullnose system safely decelerated the vehicle to a controlled stop in all 3 tests.

Figure 2.4. MwRSF Thrie-beam Bullnose Median Barrier System [7]

During phase 2 tests (MwRSF Research Report No. TRP-03-418-20), a critical limitation of the initial bullnose design was discovered during MASH 3-30 testing (test MSPBN-4). MASH Test 3-30 involved the passenger car striking the center of the nose at a 0-degree angle with a ¼-vehicle offset. In test MSPBN-4, the vehicle penetrated the system. The head-on impact, coupled with the increased kinetic energy requirements of the MASH passenger car when compared to previous NCHRP Report No. 350 test vehicles, caused the lowest thrie-beam corrugation to rupture and move downward while the upper two thrie-beam corrugations were pushed upward essentially splitting the thrie-beam rail in half along a horizontal plane. The splitting of the rail compromised the bullnose system's ability to capture the vehicle's front end and allowed it to penetrate through the barrier. In addition, contact with the rail during the test caused excessive vehicle windshield deformation, including a tear in the upper left corner. Test MSPBN-4 was deemed unacceptable under the MASH 3-30 criteria.

Following failed test MSPBN-4, researchers modified the bullnose system by adding a third retention cable behind the lowest thrie-beam corrugation in the nose section. The subsequent MASH 3-30 retest (test MSPBN-5) conducted with the modified bullnose system was successful. The passenger car was safely captured and decelerated to a controlled stop. This modification, along with the subsequent successful Phase II tests (MASH 3-31, 3-33, and 3-37b), demonstrated that the modified thrie-beam bullnose system met all requirements for MASH 2016 TL-3. The bullnose system has several similarities to the SRGS. It has a sharp curve like the SRGS and showed reliable performance under MASH TL-3 conditions. However, the bullnose has not been tested with a slope behind (or inside of) the system.

CHAPTER 3.
DESIGN AND SIMULATION ANALYSIS

3.1. INTRODUCTION

This chapter provides a detailed description of the finite element (FE) model and outlines the FE model validation process employed prior to evaluating the performance of the modified SRGS developed under NCHRP Project 15-53 when placed in front of 2:1 slope.

3.2. FINITE ELEMENT MODEL

3.2.1. Vehicle Models

For the vehicle impact simulations, the research team used a 2018 Dodge Ram 1500 pickup truck model and a 2010 Toyota Yaris passenger car model [8, 9]. These two vehicle models are publicly available and were developed by the Center for Collision Safety and Analysis (CCSA) at George Mason University. These vehicle models have been further improved by TTI researchers over a series of past research projects to achieve improved and more accurate validation. Figure 3.1shows the pickup truck and passenger car models which represent the MASH 2700P and 1100C design vehicles respectively.

(a) 2018 Dodge Ram – MASH 2270P model (b) 2010 Toyota Yaris – MASH 1100C model

Figure 3.1. FE Vehicle Models

3.2.2. SRGS Developed under NCHRP Project 15-53 Models

For simulation, the research team used the same SRGS FE model developed by George Mason University (GMU) under NCHRP Project 15-53 [2, 3]. Figure 3.2 shows the details of the SRGS FE model developed and provided by GMU. The rails were modeled with shell elements with corresponding section thickness. The piecewise linear plasticity material was used for steel components including rails. However, it should be noted that a rail rupture parameter was not included in this rail model. The cable was modeled with beam and null-shell elements for better defining contact between the cable and other system components.

(a) Overall SRGS FE model

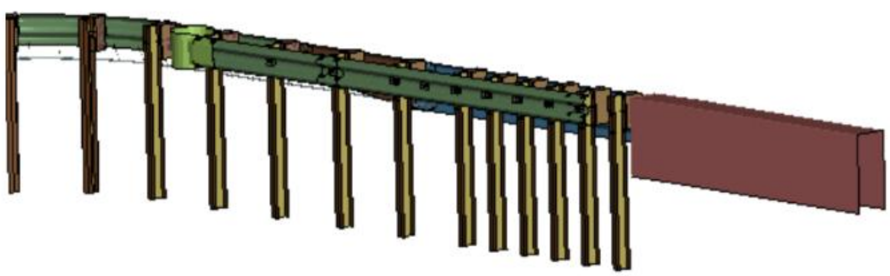

(b) Backrail Details

Figure 3.2. SRGS FE Model Developed under NCHRP 15-53

3.3. MODEL VALIDATION

A limited validation of the simulation was conducted to compare simulation results to full-scale crash tests performed under NCHRP Project 15-53 [2, 3]. The simulation was set to impact the SRGS placed in front of a 2:1 slope with a 15-degree impact angle and an impact velocity of 50 mph (80 km/h) to represent MASH Test 33 performed under NCHRP Project 15-53 (FOIL Test 20012). Figure 3.3 shows sequential images of the MASH Test 33 simulation at 50 mph (80 km/hr) performed in this study and compares it to FOIL Test 20012 conducted under NCHRP Project 15-53.

Table 3.1 lists the occupant risk factors for both the simulation and the crash test. The simulation occupant risk values were calculated and obtained by the Test Risk Assessment Program (TRAP) using the occupant risk assessment criteria specified in MASH [10]. The occupant impact velocity (OIV) and ridedown acceleration (RA) values were higher in the simulation when compared to the actual test values, while the maximum roll and pitch angles rendered by the simulation were less than the measured angles of the actual test. The reason for the different measured values is because the rail was ruptured during the crash test while the simulation model did not include a rail rupture mechanism. Due to the rail rupture, the cable - a less stiff component of the system - captured the vehicle, which allowed more deflection of the system and decreased vehicle deceleration rate. Overall, the simulation and crash test OIV, RA, and roll and pitch values were found to be reasonably close to each other. Therefore, the model was considered acceptable for use in further evaluations of the SRGS design modifications.

This validated model was then used to investigate the performance of the SRGS in front of a 2:1 slope at higher impact speeds because no full-scale MASH TL-3 crash tests exist. This analysis was necessary because the NCHRP Project 15-53 report noted that their simulations at higher speeds (56 mph (90 km/h) and 62 mph (100 km/h)) indicated “significant roll and pitch” of the vehicle which led to the project team opting to conduct the full-scale test at a lower speed of 50 mph (80 km/h). However, the project team provided no corresponding quantitative data. To bridge this gap, the model was first used to replicate the 56 mph (90 km/h) GMU simulation conducted under NCHRP Project 15-53. This functioned as a second validation step, confirming that the vehicular behaviors in terms of roll, pitch, and engagement of the rail at a higher speed followed the same trend as the GMU’s simulation as shown in Figure 3.4.

The initial 50 mph (80km/h) validation against the physical test revealed a maximum difference of 6 degrees (52% difference) in roll angle. The numerical results from the validation simulation at 56 mph (90 km/h) showed that all metrics remained within MASH limits. Critically, even if the 52% variance was applied to the 56 mph (90 km/h) roll and pitch results they would remain under MASH limits. Additionally, a simulation was conducted at the full TL-3 speed of 62 mph (100 km/h) using the validated model to establish reliable baseline values in which to evaluate the modified designs. Its numerical values were also under MASH limits, even when applying the 52% variance to the roll and pitch.

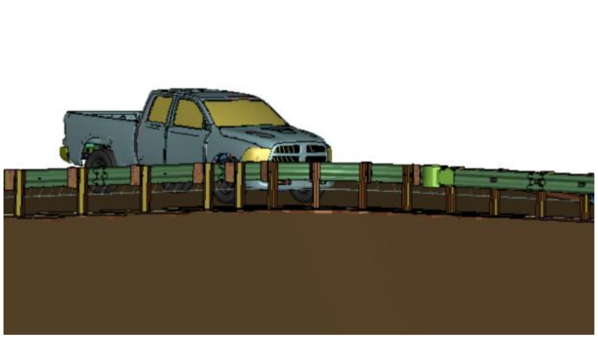

0.00 sec

0.00 sec

0.21 sec

0.21 sec

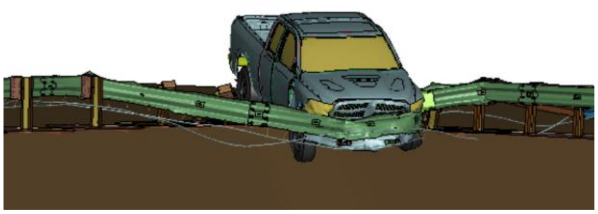

0.43 sec

0.43 sec

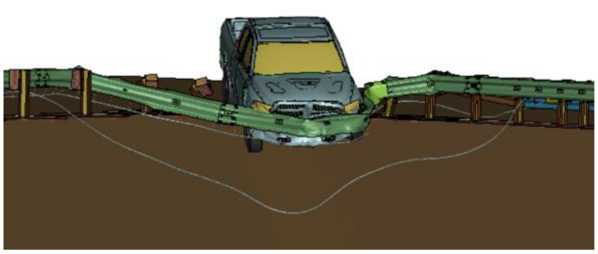

0.75 sec

0.75 sec

Figure 3.3. Sequential Images of Test 3-33 Simulation and FOIL Test 20012

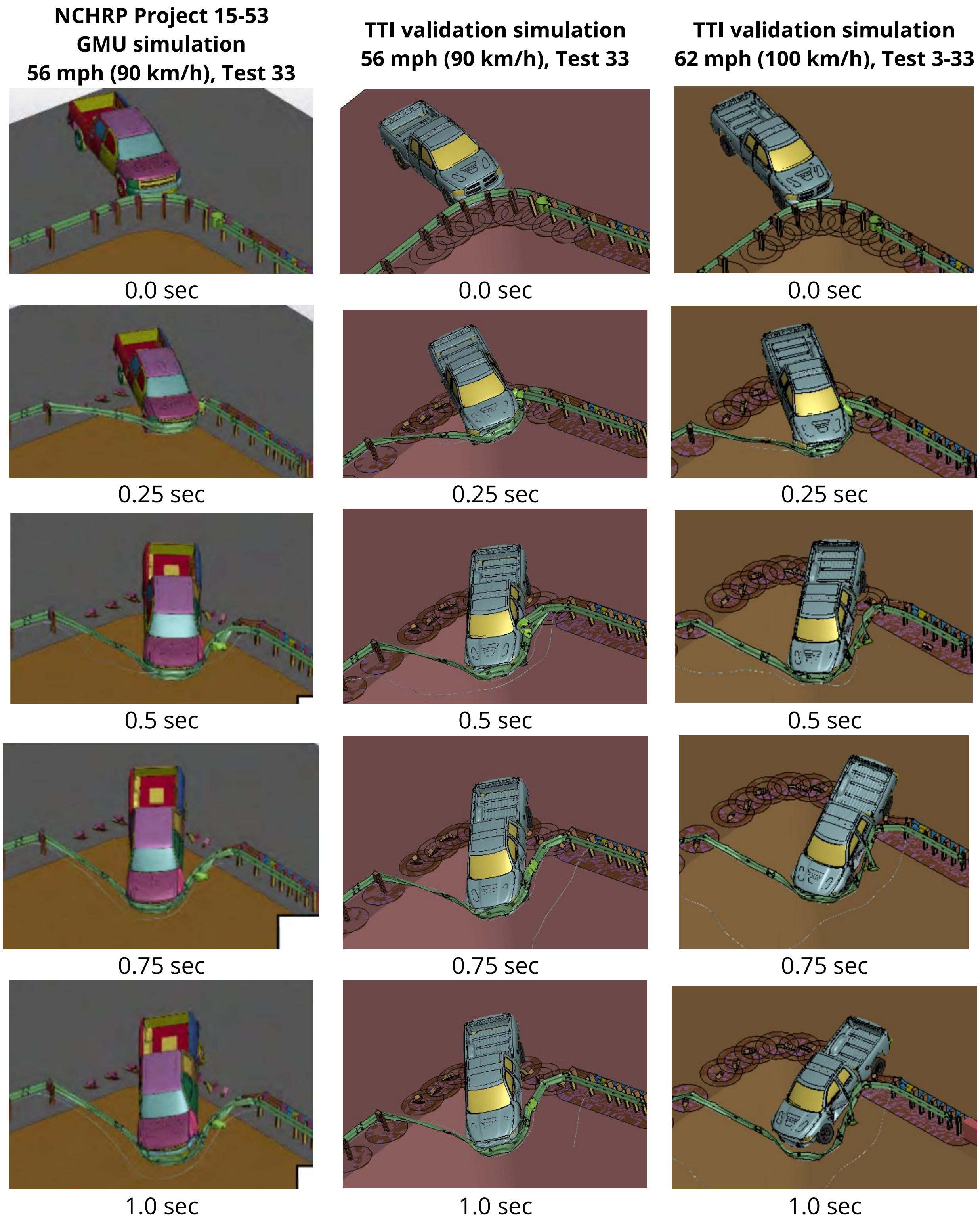

Figure 3.4. Sequential Images Comparing Simulations of Test 3-33 Performed by GMU in NCHRP Project 15-53 and TTI

Table 3.1. Occupant Risk Factors from Test 33 Simulation

		Full-Scale FOIL Test 20012 (Test 33) at 50 mph	TTI Simulation Test 33 at 50 mph	TTI Simulation Test 33 at 56 mph	TTI Simulation Test 3-33 at 62 mph
Occupant Impact Velocity (ft/s)	**X**	23.95	29.2	29.4	31.7
	Y	4.92	2.8	3.4	4.4
Ridedown Acceleration (g)	**X**	8.7	9.8	12.4	9.8
	Y	4.5	5.8	6.3	7.9
Max. Angle (degrees)	**Roll**	11.6	5.6	6.1	10.0
	Pitch	14.6	10.7	16.2	26.1
	Yaw	60.7	32.5	38.2	77.7

In summary, the FE model was validated through a two-step process. First, a simulation with an impact speed of 50 mph (80 km/h) was compared to the corresponding full-scale physical crash test, and the results were deemed "reasonably close." Next, the performance at a higher speed was verified by successfully replicating a previous 56 mph (90 km/h) simulation, which confirmed the model predicted the correct vehicle behavioral trends. Because this correlation with both physical test data and previous simulations demonstrated that the model was acceptable, the results from the 62 mph (100 km/h) simulation are considered a reliable baseline from which to evaluate future SRGS design modifications.

CHAPTER 4.
DESIGN MODIFICATION AND EVALUATION

4.1. INTRODUCTION

In this section, concepts of various design modifications to the original SRGS (developed under NCHRP Project 15-53) placed in front of a 2:1 slope were developed and evaluated under MASH TL-3 conditions. In efforts to meet MASH TL-3 criteria, selected modifications to the SRGS radius nose section included: (1) adding additional unbolted posts, (2) nesting rails, and (3) extending the flat bench section width behind posts.

4.1.1. Additional Unbolted Posts

In the first SRGS modification simulation effort, two unbolted posts were added to either side of the existing center post at the SRGS curved nose section. This modification was chosen to provide a stiffer SRGS nose section in efforts to reduce vehicle instability and minimize vehicle interaction with the 2:1 slope behind the SRGS. Figure 4.1 shows the layout of the modified SRGS FE model. Figure 4.2 shows sequential images comparing the performance of the original SRGS and the modified SRGS with additional posts under MASH TL-3 conditions.

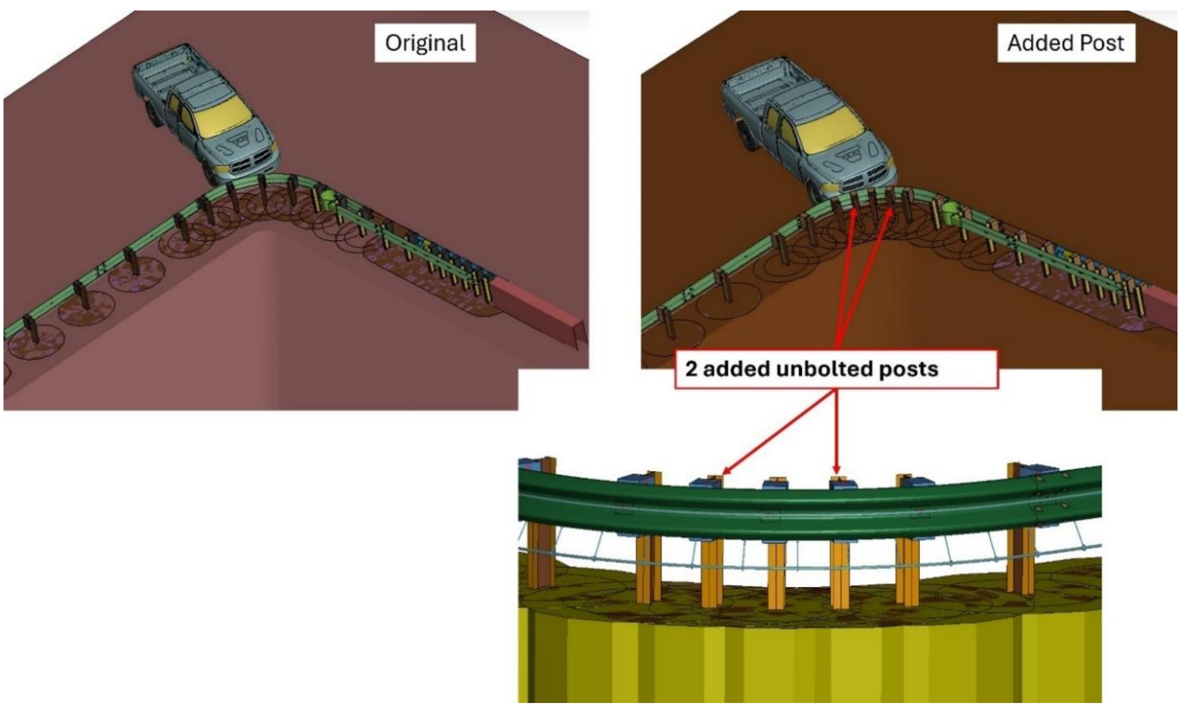

Figure 4.1. SRGS Modification: Additional Unbolted Posts Layout

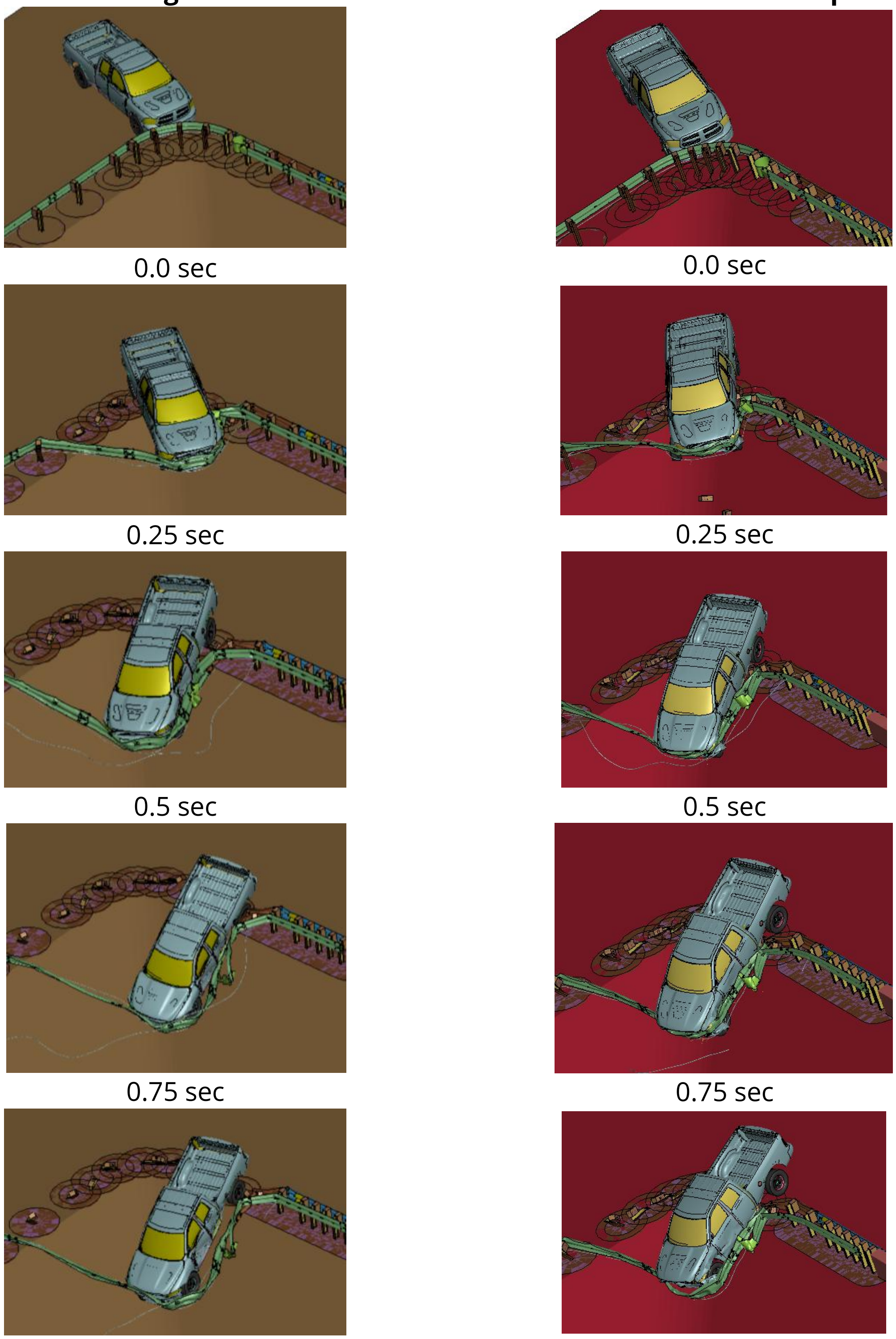

Original | Additional unbolted post

0.0 sec | 0.0 sec

0.25 sec | 0.25 sec

0.5 sec | 0.5 sec

0.75 sec | 0.75 sec

1.0 sec | 1.0 sec

Figure 4.2. Sequential Images for Test 3-33 with Additional Unbolted Posts

When comparing the sequential images, the modified system simulation was stiffer with less rail deflection. The stiffer modified system stopped and captured the vehicle before it lost stability, decelerated the vehicle quickly, and increased occupant risk factor values. Table 4.1 compares the occupant risk factors between the original design and the additional posts simulation. Even though the maximum OIV and RA values increased, they were still under the allowable MASH limits while the maximum roll and pitch angles were lower than the original design which indicates increased vehicle stability.

Table 4.1. Occupant Risk Factors for Test 3-33 with Additional Unbolted Post

		Original design	Additional Post	MASH-16 Limit
Occupant Impact Velocity (ft/s)	**X**	31.7	35.6	40
	Y	4.4	6.3	40
Ridedown Acceleration (g)	**X**	9.8	10.9	20.49
	Y	7.9	4.3	20.49
Max. Angle (degrees)	**Roll**	10.0	9.5	75
	Pitch	26.1	20.8	75
	Yaw	77.7	63.9	N/A

4.1.2. Nested Beam

In the second SRGS modification simulation, the SRGS rails were nested at the nose section in efforts to increase the nose stiffness, reduce vehicle instability, and minimize vehicle interaction with the 2:1 slope behind the SRGS. Figure 4.3 shows the layout of the modified SRGS FE model. The SRGS with the nested beam simulations were evaluated for both the 10-gauge and 12-gauge rails. Figure 4.4 shows sequential images comparing performance of the original SRGS to the modified SRGS with the nested beams under MASH TL-3 conditions.

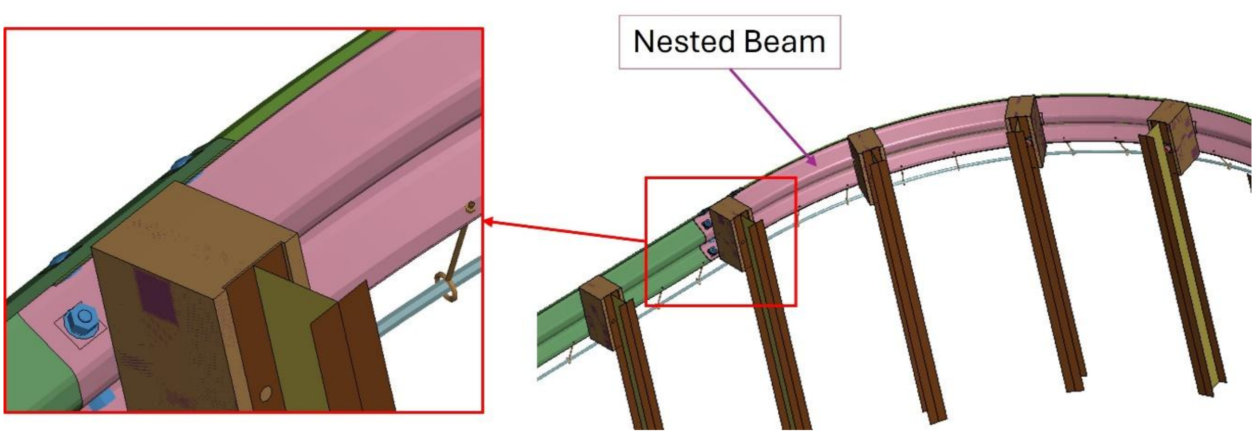

Figure 4.3. SRGS Modification: Nested Rails at the Nose Layout

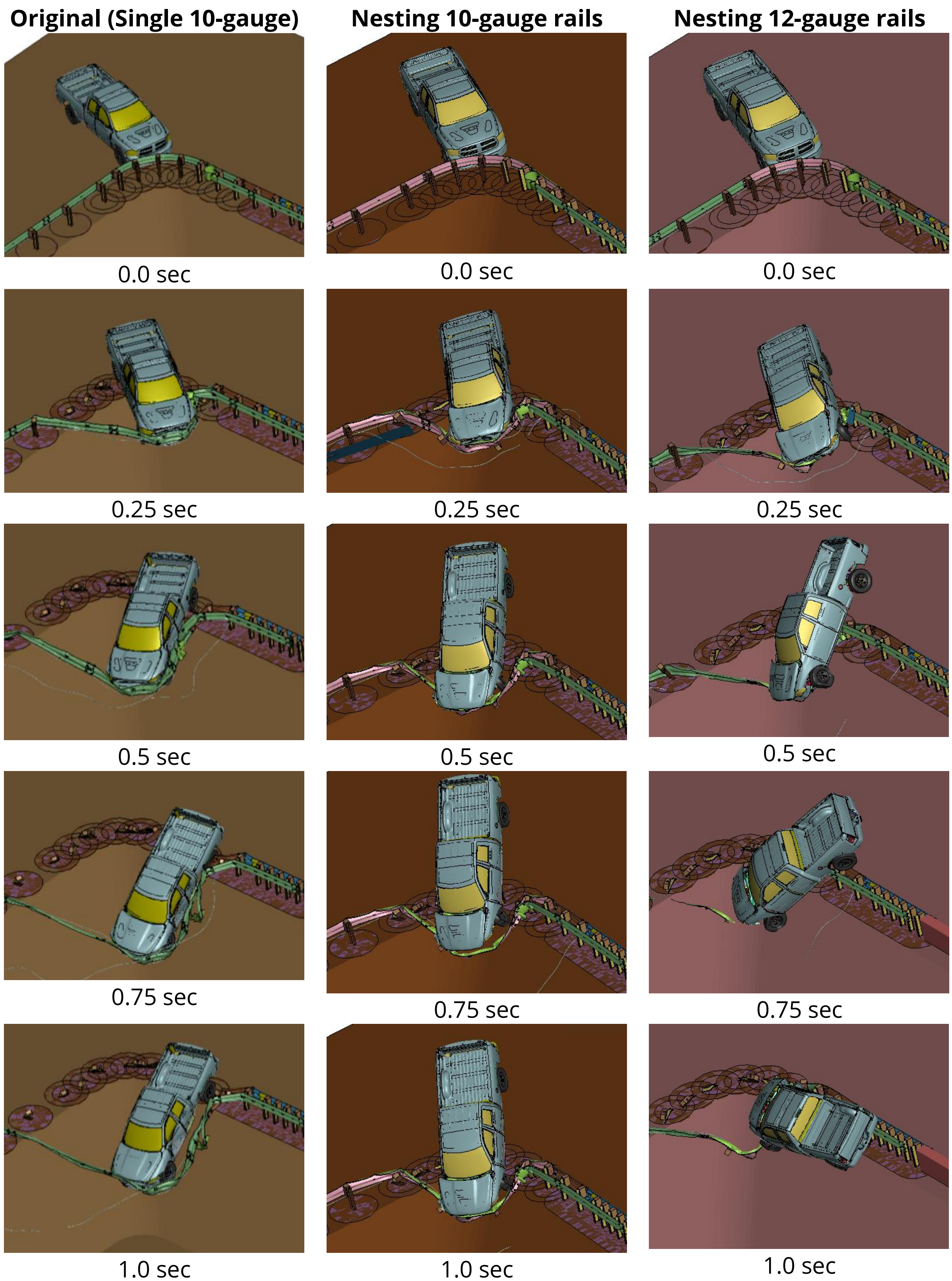

Figure 4.4. Sequential images for Test 3-33 with Nested Nose Rails

As seen in the sequential images of Figure 4.4, the nested rail system introduced excessive stiffness at the nose. This over-stiffening resulted in an abrupt, high-magnitude deceleration of the vehicle inducing severe roll and pitch angles for both 10- and 12-gauge modification simulations. The resulting vehicle instability caused the pickup truck to override the barrier for both 10- and 12-gauge simulations and subsequently roll onto the slope for the 12-gauge rail simulation. The occupant risk factors in Table 4.2 show that OIV, RA, and vehicle roll and pitch angles were significantly higher for the nested beam system when compared to the original design. Due to concerns about elevated occupant risk factors and vehicle instability, this design modification was eliminated from further consideration.

Table 4.2. Occupant Risk Factors for Test 3-33 with Nested Beam

		10-gauge Single Layer (original)	**10-gauge Nested Rail**	**12-gauge Nested Rail**	**MASH-16 Limit**
Occupant Impact Velocity (ft/s)	X	31.7	36.5	33.1	40
	Y	4.4	1.0	2.6	40
Ridedown Acceleration (g)	X	9.8	15.2	12.9	20.49
	Y	7.9	13.4	6.4	20.49
Max. Angle (degrees)	Roll	10.0	17.3	41.8	75
	Pitch	26.1	42.5	42.1	75
	Yaw	77.7	29.8	191*	N/A

* *Vehicle overrides the rail*

4.1.3. Flat Bench Extension

For the third SRGS modification simulation, the SRGS was modified to have an extended flat bench section behind the posts to reduce vehicle instability by minimizing vehicle interaction with the 2:1 slope behind the SRGS. In this study, the original 2-ft flat bench section width for the SRGS was extended to 3-, 4-, and 5-ft in widths in efforts to identify the width that provides the greatest level of vehicle stability and improve the crashworthiness of the system. Figure 4.5 shows the 2-ft flat bench of the original SRGS and the wider 3-, 4-, and 5-foot flat benches of the modified SRGS systems.

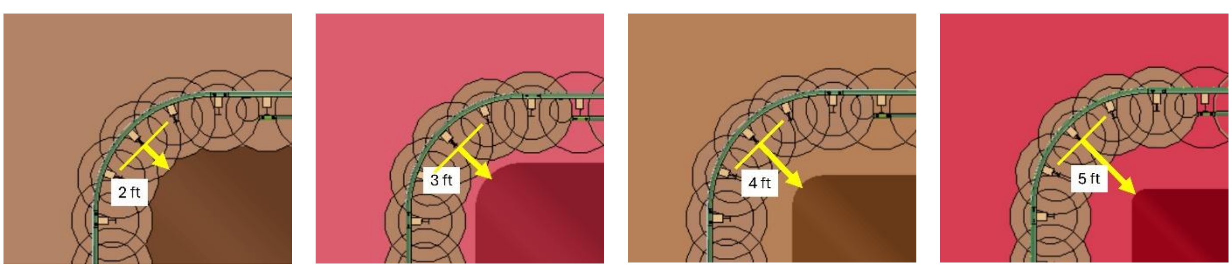

Figure 4.5. SRGS Modification: Different Flat Bench Widths behind Posts

As mentioned in Chapter 2 of this report, NCHRP project 15-53 previously investigated the performance of the initial SRGS design using FE simulations with various flat bench section widths and slopes varying from 6:1 to 2:1. Those simulations, which modeled the SRGS without a W-beam backrail (see Figure 2.1), concluded that the only configuration in front of a 6:1 slope was likely to pass MASH TL-3 tests for both vehicles. Please note that the back rail was not a part of the initial SRGS design but was added to the SRGS during the crash testing phase to increase system stiffness after the original SRGS failed MASH Test 3-33 on flat ground. Subsequently, the modified SRGS with the back rail successfully passed MASH Test 3-33 on flat ground and established it as the current baseline MASH TL-3 compliant design.

As a result, a direct performance comparison of the SRGS with and without the back rail in front of a 2:1 slope with a 2-ft bench section was not conducted in NCHRP Project 15-53. Therefore, this study performed and compared the baseline simulations of these two system configurations (illustrated in Figure 4.6) of with and without backrail in front of a 2:1 slope. This purpose of this comparison was to confirm that the SRGS with the backrail improves upon and overcomes the performance issues observed in earlier simulations of the initial SRGS design when placed in front of varying slopes. In confirming this improvement, it provides the necessary justification to evaluate further design modifications of extending the flat bench section width.

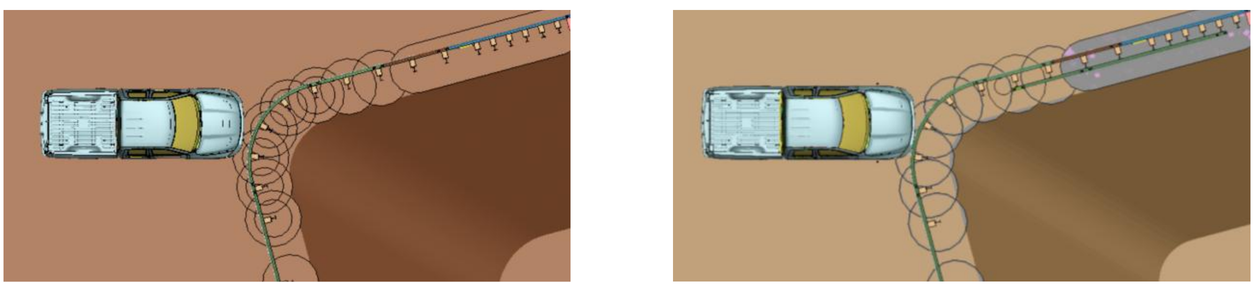

Without backrail With backrail

Figure 4.6. Test 3-33 Setup without and with Backrail

Figure 4.7 provides a sequential comparison of the baseline simulations performed without and with the backrail. The images show significantly reduced rail deflection and enhanced vehicle stability for the SRGS with backrail in front of a slope, particularly at 0.5 seconds and 0.75 seconds. This improved performance is due to the increased system stiffness provided by the backrail which enables the SRGS to effectively contain the vehicle and mitigate vehicle instability induced by high roll and pitch motions.

Table 4.3 shows occupant risk factors from both simulations. The addition of the backrail increased system stiffness, which resulted in a slight increase in maximum RA. Conversely, vehicle stability factors improved significantly in all categories for the SRGS with a backrail. Most notably, the maximum roll angle was reduced by 39.5 degrees. Therefore, the results provided the rationale to further evaluate the performance of a wider flat bench for the system with the backrail.

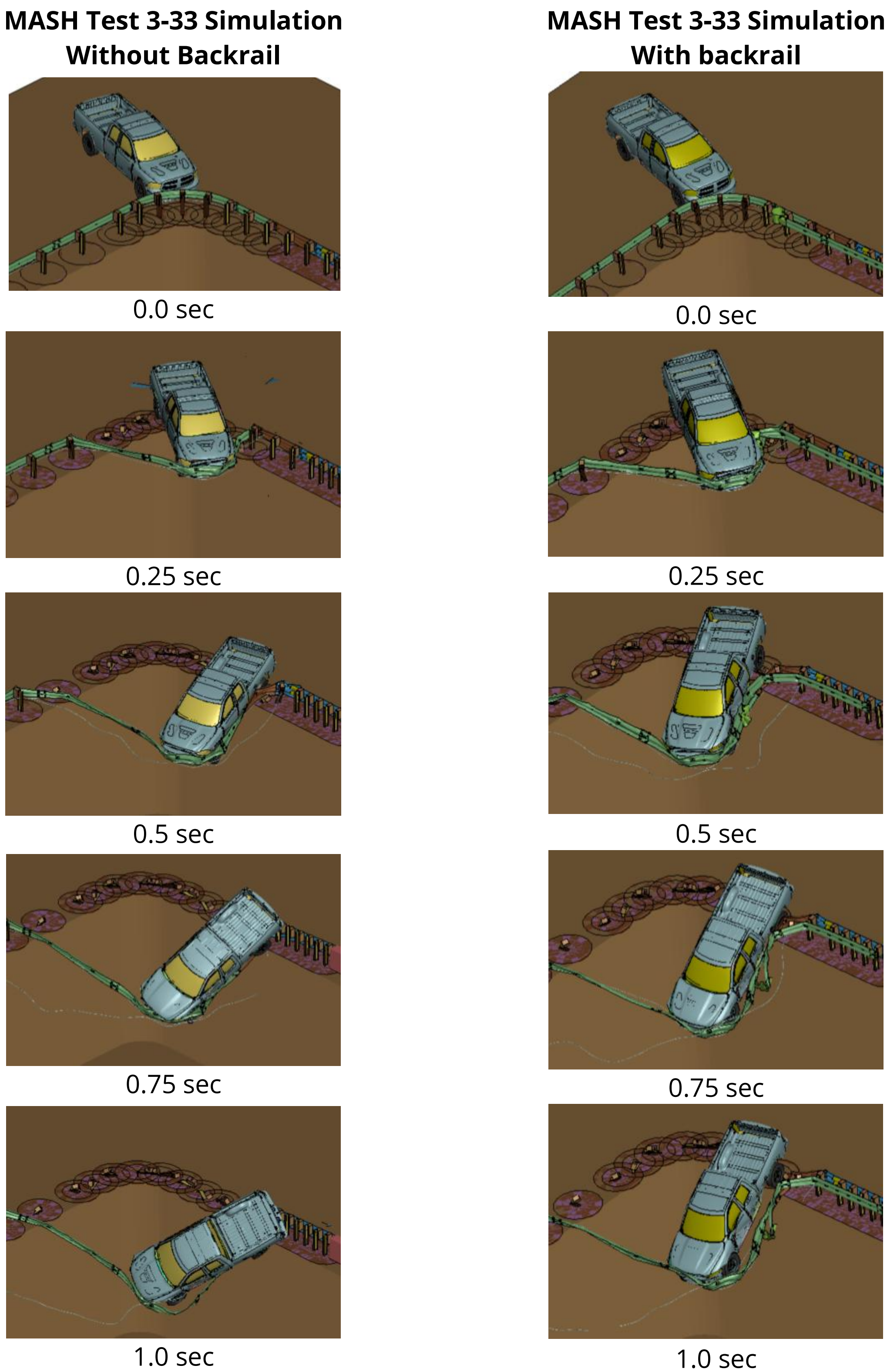

Figure 4.7. Sequential Images for MASH Test 3-33 Simulation of SRGS without and with W-beam Backrail

Table 4.3. Occupant Risk Factors for MASH Test 3-33 without and with Backrail

		Without Backrail	With Backrail	MASH-16 Limit
Occupant Impact Velocity (ft/s)	X	31.1	31.7	40
	Y	4.8	4.4	40
Ridedown Acceleration (g)	X	7.3	9.8	20.49
	Y	8.1	7.9	20.49
Max. Angle (degrees)	Roll	49.5	10.0	75
	Pitch	33.0	26.1	75
	Yaw	145.8*	77.7	NA

* *Vehicle overrides the rail*

Based on findings from these baseline simulations, the widening of the flat bench option was chosen to be evaluated as one of the potential design modifications for the SRGS with a W-beam backrail in front of a 2:1 slope. Figure 4.8 presents sequential images from simulations comparing overall system performance and vehicle behaviors for four different flat bench widths: 2-ft (original), 3-ft, 4-ft, and 5-ft. The simulations demonstrate a correlation between greater flat bench width and increased vehicle stability. In the original design with a 2-ft flat bench width, the front half of the vehicle dropped off the edge of the flat bench at 0.5 seconds after initial impact. This drop induced a severe pitch that increased through the 1.0 second mark, indicating a high risk of vehicle flipping. However, the wider flat bench section simulations indicated an improvement in vehicle stability with lower pitch angles as the flat bench width increased.

The trend is quantified by the occupant risk factors presented in Table 4.4. As the flat bench width increases to 5-ft, the vehicle’s roll and pitch angles decrease, which is a key indicator of improved vehicle stability.

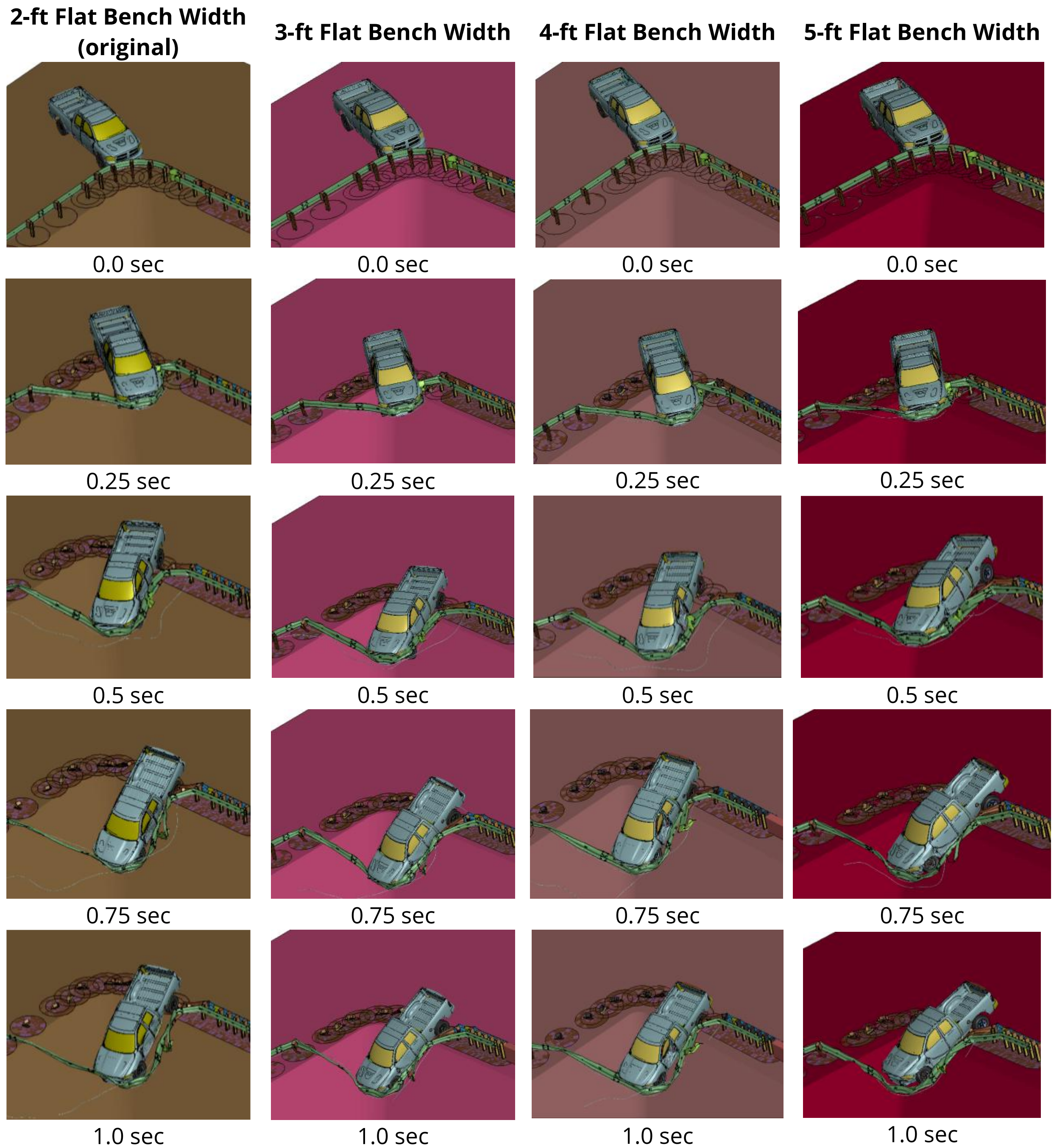

Figure 4.8. Sequential Images for Test 3-33 with Extended Flat Bench Section

Table 4.4. Occupant Risk Factors for Test 3-33 with Extended Flat Bench Section

		2-ft – (original)	3-ft	4-ft	5-ft	MASH-16 Limit
Occupant Impact Velocity (ft/s)	X	30.6	31.3	30.8	31.9	40
	Y	5.3	6.0	5.1	5.0	40
Ridedown Acceleration (g)	X	9.9	10.8	8.9	10.2	20.49
	Y	8.2	7.6	8.0	6.4	20.49
Max. Angle (degrees)	Roll	7.1	7.4	6.7	6.5	75
	Pitch	30.5	28.3	23.3	22.5	75
	Yaw	64.6	80.0	69.1	79.1	NA

4.2. FURTHER SIMULATION

Following the MASH Test 3-33 simulations to evaluate different modified system designs, the modification to widen the flat bench section was selected for further evaluation after discussion with the project technical representatives. This approach avoids direct changes to the system model and was also chosen because the original FE model was not developed by TTI researchers. Modifying an externally developed model introduces significant uncertainty and reduces confidence in the subsequent simulation results despite the prior SRGS validations.

The project researchers determined that a subsequent set of MASH Test 3-32 simulations would be performed to further evaluate the performance of the modified system. These simulations assessed both the occupant risk factors and SRGS structural integrity using the passenger car model under MASH Test 3-32 conditions.

4.2.1. Test 3-32 Simulation on the SRGS with Extended Flat Bench Section

Simulations with the passenger car were performed for the original 2-ft flat bench width as well as for the 3-ft and 4-ft configurations under MASH Test 3-32 conditions. Figure 4.9 shows the sequential images comparing the results of the simulations with the three different flat bench widths. When comparing simulations of the 2-ft and 3-ft flat bench widths to the 4-ft flat bench width, the 4-ft flat bench width simulation results indicated as being the most likely width able to successfully capture the vehicle before the vehicle lost stability.

The occupant risk factors presented in Table 4.5 corroborate the sequential image analysis in terms of vehicle stability. As the flat bench width increases, the maximum roll angle consistently decreases from 22.2 degrees to 16.0 degrees as an indicator of improved vehicle stability. In terms of occupant risk factors, the longitudinal OIV consistently decreased from 43.5 ft/s to 38.8 ft/s as the flat bench increased in width.

Although the RA values did not follow a linear trend, the final 4-ft configuration yielded lower maximum accelerations when compared to the original 2-ft design (17.3 g vs. 20.6 g).

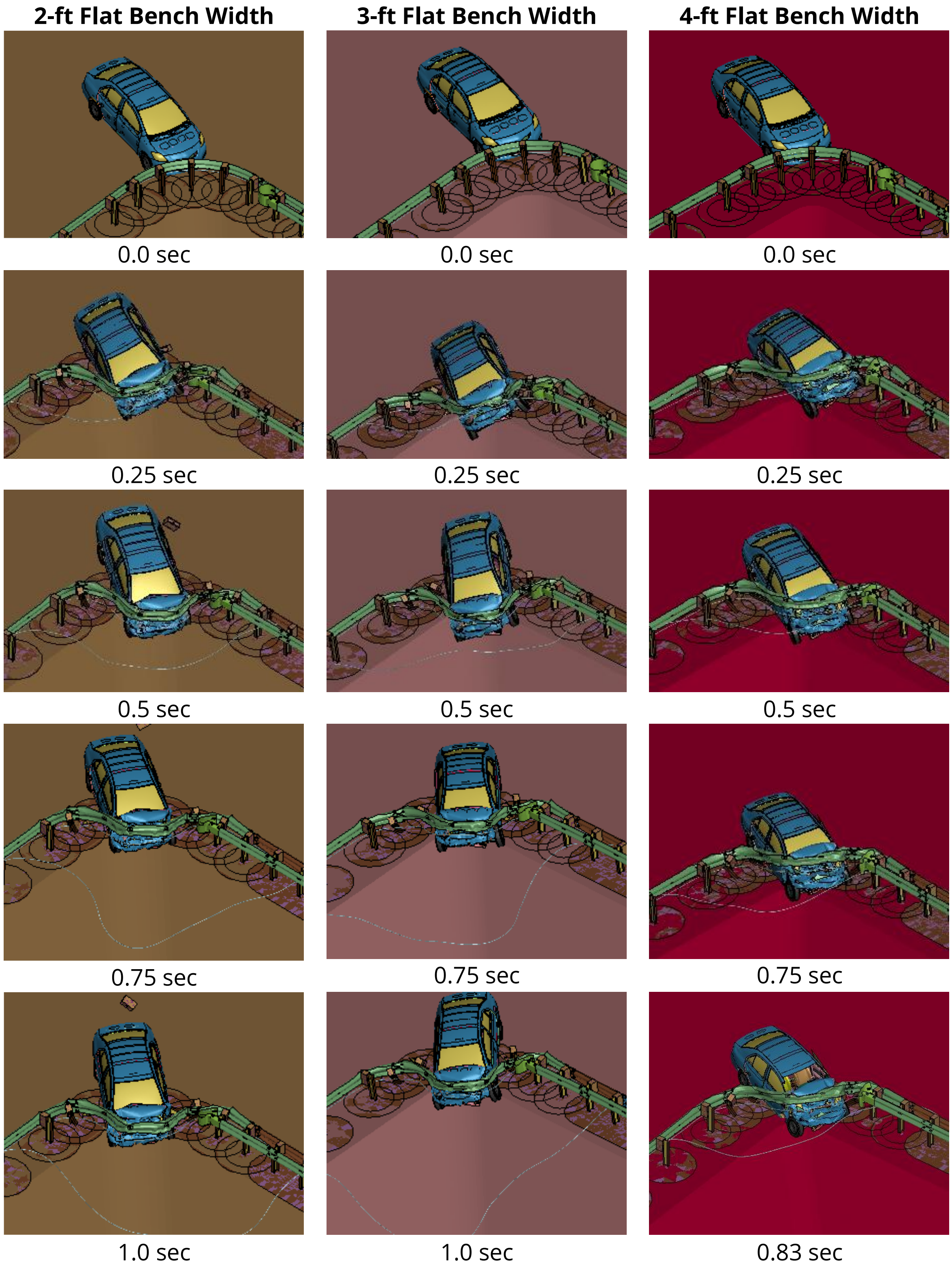

Figure 4.9. Sequential Images for Test 3-32 with Extended Flat Bench Section

Table 4.5. Occupant Risk Factors for Test 3-32 with Extended Flat Section

		2-ft (original)	3-ft	4-ft	MASH-16 Limit
Occupant Impact Velocity (ft/s)	**X**	43.5	42.4	38.8	40
	Y	0.1	2.0	2.2	40
Ridedown Acceleration (g)	**X**	20.6	15.6	17.3	20.49
	Y	6.5	6.8	5.8	20.49
Max. Angle (degrees)	**Roll**	22.2	19.0	16.0	75
	Pitch	5.8	10.7	6.4	75
	Yaw	7.0	32.5	5.8	N/A

4.2.2. Critical Impact Angle

To establish the most critical impact scenario for the SRGS, a comparative analysis for different impact angles was also performed. This was deemed necessary since no specific MASH test matrix exists for an SRGS. While NCHRP Report 15-53 [1] used a 15-degree impact angle by treating the SRGS as a terminal, the SRGS also functions as a longitudinal barrier. This suggests that a steeper 25-degree angle could represent a more severe impact. Therefore, simulations were performed using both a pickup truck and passenger car to represent modified MASH Tests 3-33 and 3-32 at a 25-degree impact angle. Figure 4.10 Shows the modified impact angle setup for Tests 3-33 and 3-32.

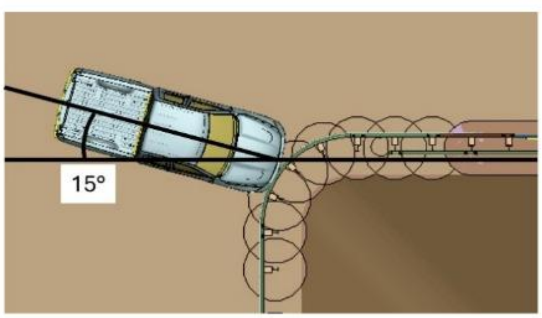

(a) Test 3-33

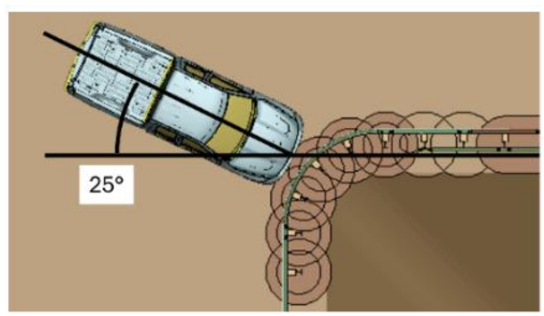

(b) Modified Test 3-33

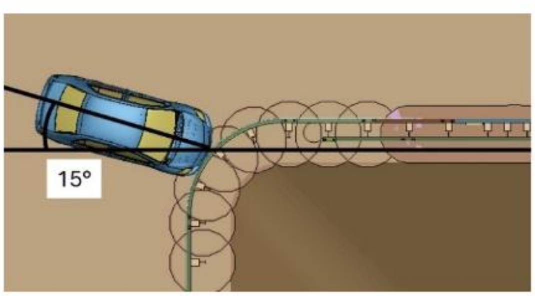

(c) Test 3-32

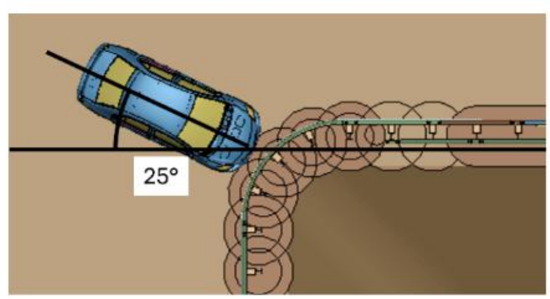

(d) Modified Test 3-32

Figure 4.10. Modified Tests 3-33 and 3-32 Setup with 25-degree Impact Angle

To compare the criticality of the two impact angles, the project team first evaluated the original SRGS developed under NCHRP Project 15-53 with 2-ft flat bench section in front of a 2:1 slope. Figure 4.11 and Figure 4.12 show sequential images for both the pickup truck and passenger car tests comparing criticality of the impact angles under MASH TL-3 impact conditions with a 62 mph (100km/h) impact speed.

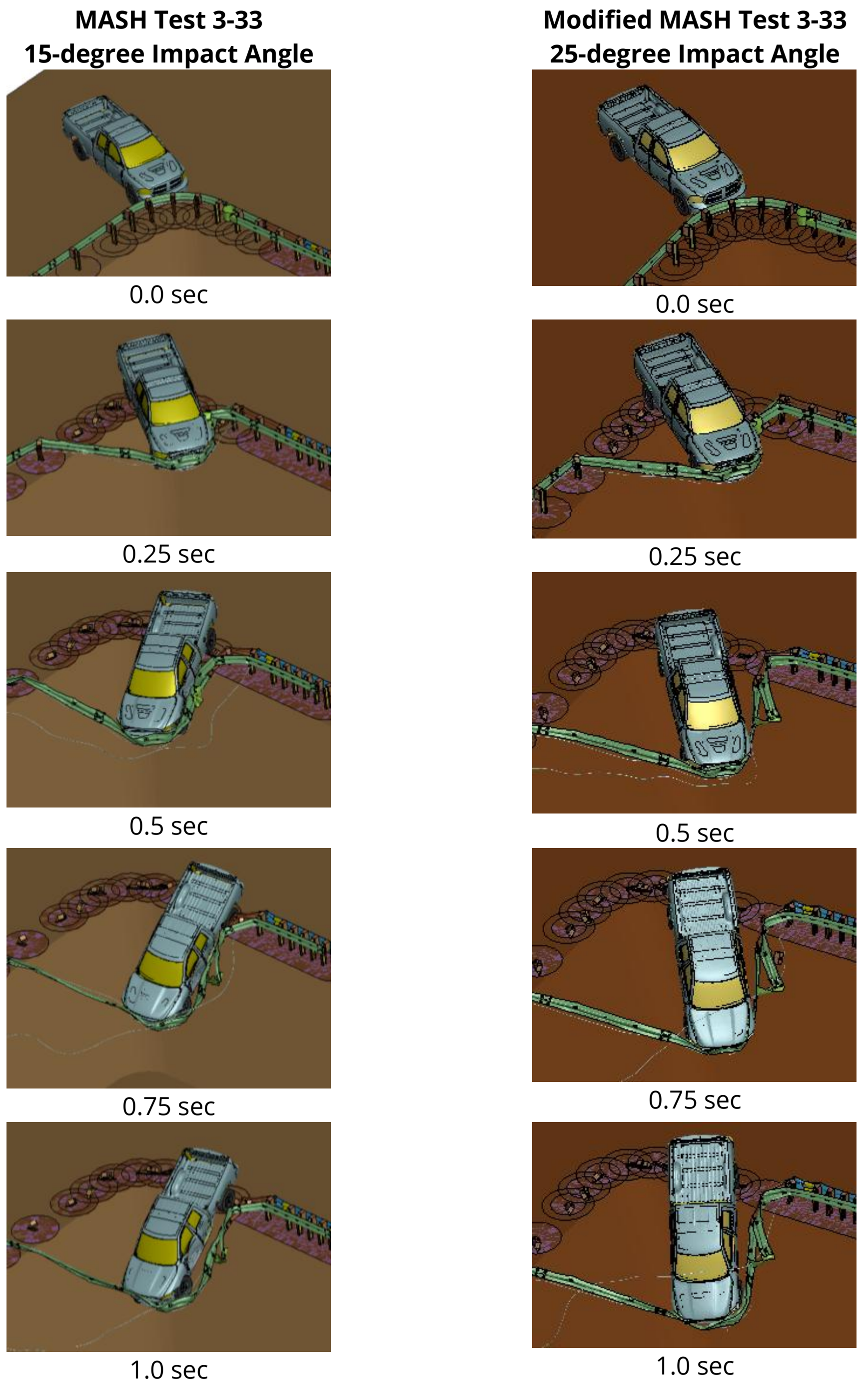

Figure 4.11. Sequential Images Comparing Test 3-33 with 15-Degree and 25-Degree Impact Angles

MASH Test 3-32 15-degree Impact Angle | **Modified MASH Test 3-32 25-degree Impact Angle**

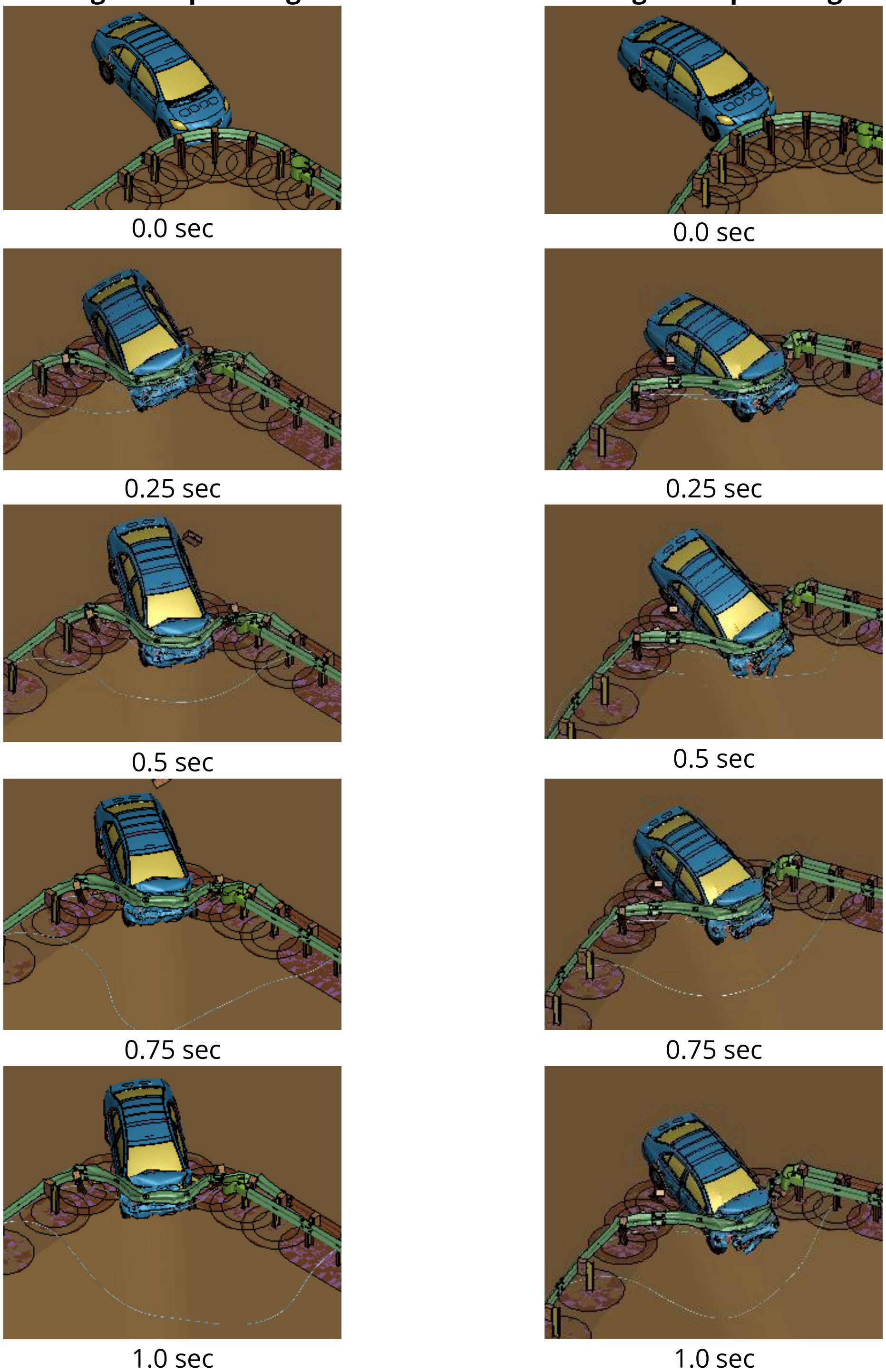

Figure 4.12. Sequential Images Comparing Test 3-32 and with 15-Degree and 25-Degree Impact Angles

Table 4.6 presents the occupant risk factors for these simulations. The 25-degree impact angle indicates greater vehicle instability as shown by the increased pitch angles.

Table 4.6. Occupant Risk Factors Comparing Effect of Different Impact Angles

		Pickup Truck 15-degrees	Pickup Truck 25-degrees	Passenger car 15-degrees	Passenger car 25-degrees	MASH-16 Limit
Occupant Impact Velocity (ft/s)	X	31.7	28.2	43.5	39.5	40
	Y	4.4	3.5	0.1	1.7	40
Ridedown Acceleration (g)	X	9.8	9.5	20.6	12.0	20.49
	Y	7.9	6.5	6.5	6.0	20.49
Max. Angle (degrees)	Roll	10.0	7.6	22.2	19.5	75
	Pitch	26.1	*43.9*	5.8	16.0	75
	Yaw	77.7	40.4	7.0	11.2	N/A

4.2.3. Evaluation on Modified SRGS Design with 4 ft Flat Section with Modified Impact Angle

Based on the initial simulations with the modified 25 degrees impact angle, which showed 25 degrees is more critical for the SRGS, the project team ran additional extended flat bench simulations to further evaluate the SRGS performance with the 25 degrees impact condition. Figure 4.13 shows test setups with a modified impact angle of 25 degrees on the modified SRGS with a 4-ft flat bench width.

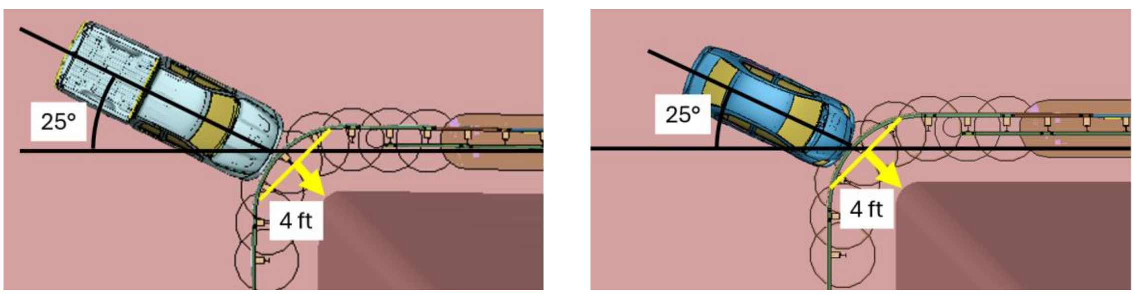

Figure 4.13. Modified Tests 3-33 and 3-32 Setup on SRGS with 4-ft Flat Bench

To evaluate the modified SRGS with the extended flat bench width at 25 degrees, the SRGS with the 4-ft flat bench width was evaluated at different impact angles of 15 degrees (original) and 25 degrees (modified) for both the pickup truck and the passenger car. Figure 4.14 and Figure 4.15 show sequential images comparing the simulations with different impact angles (15 degrees vs. 25 degrees) for Test 33 (pickup truck) and Test 32 (passenger car), respectively. Table 4.7 shows occupant risk factors for the modified SRGS test simulations with a 4-ft extended flat bench section being impacted at 15- and 25 degrees with the pickup truck and passenger car.

For the pickup truck, the increasing impact angle from 15 degrees to 25 degrees decreased the vehicle stability in roll and pitch at around 0.5 seconds through 1.0 seconds after impacting the system. The OIV, RA, and vehicle stability values were all under the MASH-16 acceptable limits.

15-degrees with 4-ft Flat Bench Width **25-degrees with 4-ft Flat Bench Width**

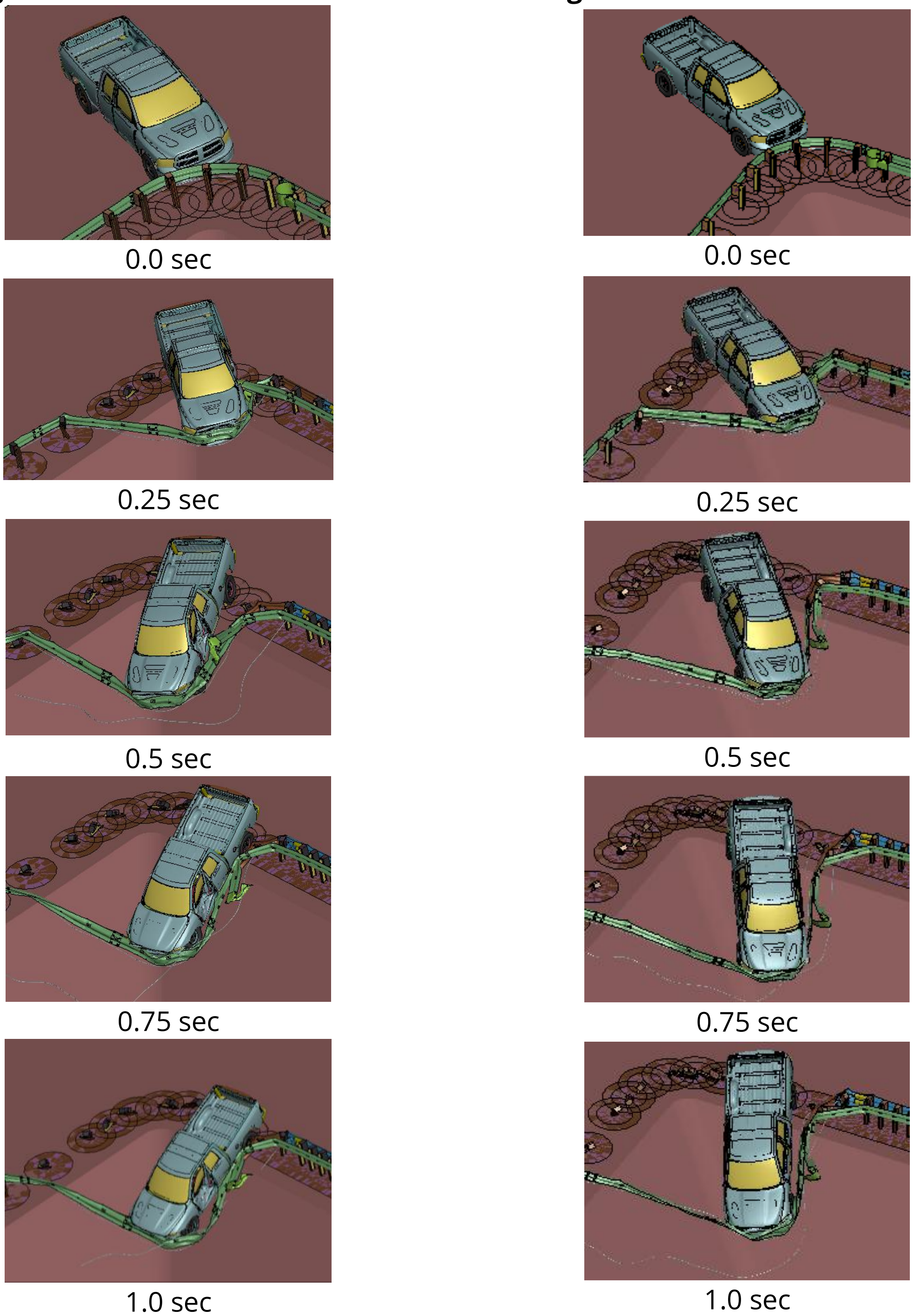

Figure 4.14. Sequential Images for Pickup Truck impacting SRGS with 4 ft Flat Bench Section at 15- and 25-Degrees

For the passenger car, the stability of the vehicle impacting the SRGS at 25 degrees was decreased with a greater pitch angle when comparing it to 15-degree impacts. However, all occupant risk values were under the MASH-16 acceptable limits.

15-degrees with 4-ft Flat Bench Width **25-degrees with 4-ft Flat Bench Width**

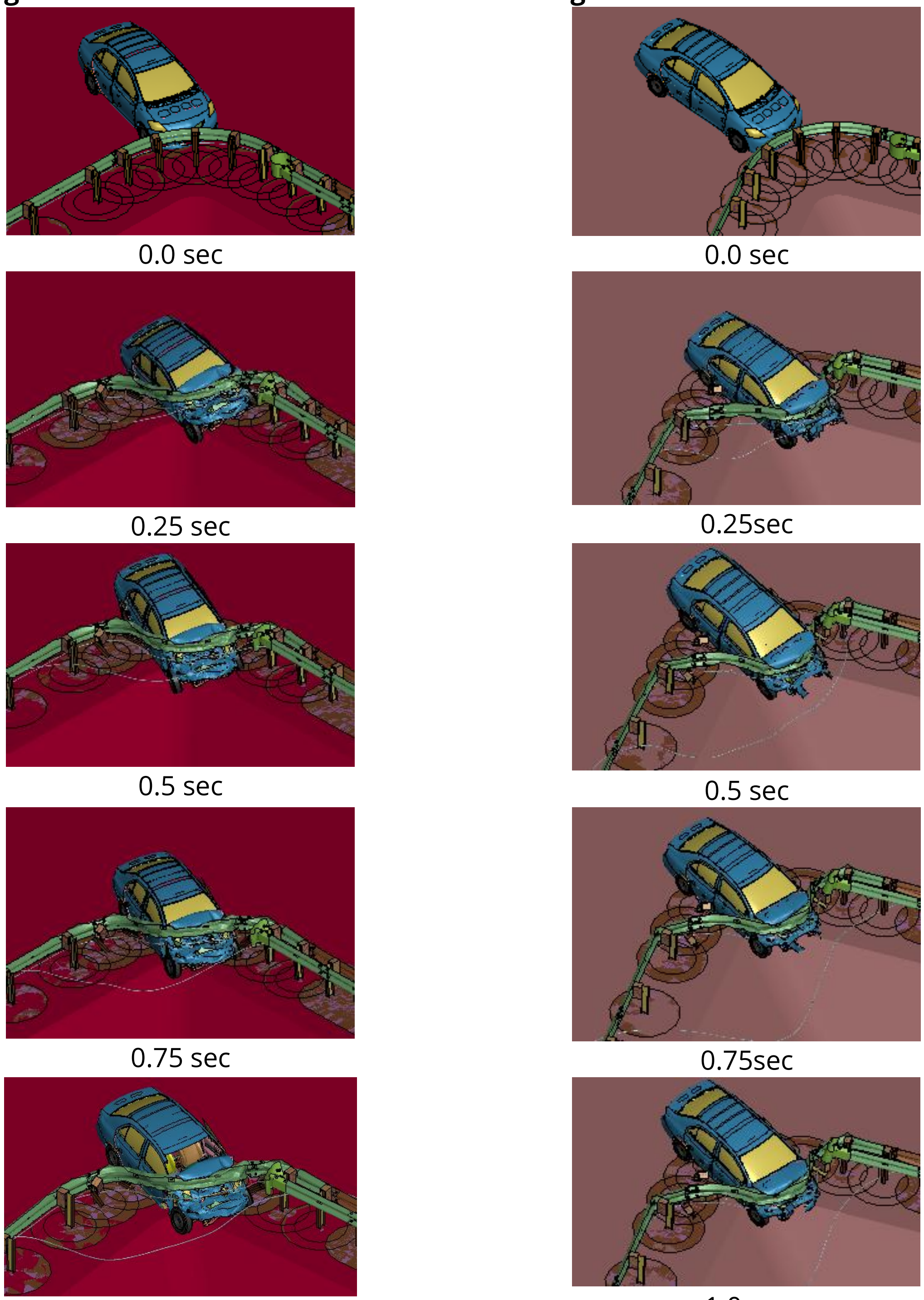

Figure 4.15. Sequential Images for Passenger Car impacting SRGS with 4-ft Flat Bench Section at 15- and 25-Degrees

Table 4.7. Occupant Risk Factors for the Modified SRGS with 4ft Flat Bench and Vehicle Impacting Angle of 15- and 25-Degrees

		Pickup Truck 15 degrees	**Pickup Truck 25 degrees**	**Passenger car 15 degrees**	**Passenger car 25 degrees**	**MASH-16 Limit**
Occupant Impact Velocity (ft/s)	X	30.8	28.2	38.8	39.9	40
	Y	5.1	4.3	2.2	0.4	40
Ridedown Acceleration (g)	X	8.9	11.5	17.3	13.8	20.49
	Y	8.0	6.2	5.8	5.7	20.49
Max. Angle (degrees)	Roll	6.7	11.2	16.0	11.2	75
	Pitch	23.3	31.5	6.4	9.0	75
	Yaw	69.1	42.5	5.8	4.7	N/A

In summary, at a 25-degree impact angle, the vehicle stability was worse for both the pickup truck and passenger car, as observed in the sequential image analysis along with increased pitch and/or roll angles. For OIV and RA, the maximum values were increased when impacting the SRGS at 25 degrees. However, all occupant risk values are still below the MASH allowable limits, indicating the modified SRGS system can meet MASH crash testing criteria for both a passenger car and a pickup truck.

CHAPTER 5.
SUMMARY AND DISCUSSION

This study evaluated several potential SRGS modifications in efforts to find a MASH TL-3 compliant SRGS when placed in front of a 2:1 slope. Simulations for several different modified SRGS designs were performed under MASH TL-3 impact conditions to evaluate the after-impact behavior of the system and the vehicle stability. In this study, the test matrix for the terminal or crash cushion was used, which includes impacting the system nose at an impact angle of 15 degrees. This impact angle was adopted (like previous SRGS studies) because no test matrix exists for an SRGS, and an SRGS acts somewhat like a terminal or crash cushion. Simulations were run to specifically evaluate SRGS performance under MASH Tests 3-32 and 3-33 criteria.

This study evaluated the following potential modifications: (1) an extended flat bench width at 3-, 4-, and 5-ft widths, (2) additional unbolted posts in the SRGS nose section, and (3) 10- and 12-gauge nested radius rail configurations (see Figure 5.1). Ultimately, the modification with 4-ft flat bench width was selected as the SRGS design most likely to meet MASH TL-3 crash testing criteria while minimizing significant modifications to the originally tested SRGS system.

After selecting the widened flat bench width modification, the impact angle was adjusted from 15 degrees to 25 degrees because the SRGS also functions as a longitudinal barrier in addition to acting as a terminal.

For the final analysis step, this study evaluated the modified SRGS with a 4-ft flat bench section under MASH TL-3 conditions impacting at a 25 degrees impact angle.

Extended Bench Setup **2 Added Post Setup** **Nested Beam Setup**

Figure 5.1. SRGS Design Modification Options

Table 5.1 compares the occupant risk factors of Test 3-33 for the original SRGS configuration and different potential design modifications including the extended 4-ft flat bench section, additional posts, and nested 10- and 12-gauge rail options. The extended 4-ft flat bench section produced results generally comparable to the original design with reductions in longitudinal OIV, RA, and roll and pitch angles. The additional-post configuration indicated increased OIV but showed reduced pitch angles when compared to the original design. The 10-gauge nested beam configuration indicated the highest longitudinal OIV and RA values as well as increased roll and pitch angles. The 12-gauge nested beam showed somewhat lower OIVs than the 10-gauge nested rail but resulted in the vehicle overriding with the largest roll and yaw angles of all configurations. Overall, the extended 4-ft flat bench section provided the most balanced performance among all the evaluated modifications and was chosen for further evaluation.

Table 5.1. Occupant Risk Factors Comparison: SRGS Design Modifications of Test 3-33

		Original (NCHRP 15-53)	Extended Flat Bench Width (4-ft)	Additional Posts	Nested Beam (10-gauge)	Nested Beam (12-gauge)
OIV (ft/s)	X	31.7	30.8	35.6	36.5	33.1
	Y	4.4	5.1	6.3	1.0	2.6
RA (g)	X	9.8	8.9	10.9	15.2	12.9
	Y	7.9	8.0	4.3	13.4	6.4
Max. Angle (degrees)	Roll	10.0	6.7	9.5	17.3	41.8
	Pitch	26.7	23.3	20.8	42.5	42.1
	Yaw	77.7	69.1	63.9	29.8	191*

* *Due to vehicle overriding*

Next, the SRGS with the 4-ft flat bench section was further evaluated through additional computer simulations under MASH Test 3-32 impact conditions with a passenger car. Table 5.2 provides the occupant risk factors comparing the original system with a 2-ft flat bench section to the modified system with an extended 4-ft flat bench section. Overall, the 4-ft flat bench section improved system performance in terms of occupant risk and vehicle stability when compared to the original 2-ft flat bench width for Test 3-32. The maximum OIV decreased from 43.5 ft/s to 38.8 ft/s while the maximum RA decreased from 20.6 g to 17.3 g. Vehicle stability was increased with the maximum roll angle being reduced from 22.2 degrees to 16.0 degrees with the 4-ft flat bench section.

Table 5.2. Occupant Risk Factors Comparison: Bench Extension of Test 3-32

		2-ft flat bench section (original)	4-ft flat bench section
Occupant Impact Velocity (ft/s)	X	43.5	38.8
	Y	0.1	2.2
Ridedown Acceleration (g)	X	20.6	17.3
	Y	6.5	5.8
Max. Angle (degrees)	Roll	22.2	16.0
	Pitch	5.8	6.4
	Yaw	7.0	5.8

Table 5.3 summarizes the occupant risk factors for the SRGS with modified Tests 3-32 (passenger car) and 3-33 (pickup truck) at a 25 degrees impact angle and comparing 2-ft and 4-ft flat bench section widths. For the passenger car, increasing the flat bench width from 2-ft to 4-ft produced slight improvements in vehicle stability. Simulations showed reductions in roll angle from 19.5 to 11.2 degrees, reductions in pitch angle from 16.0 to 9.0 degrees, and the maximum OIVs remained nearly unchanged. For the modified Test 3-33 with the pickup truck, the 2-ft and 4-ft flat bench widths showed similar maximum OIVs of 28.2 ft/s, a reduced pitch angle from 43.9 to 31.5 degrees, and a slightly increased roll angle from 7.6 to 11.2 degrees. Overall, simulations indicate that even when impacting at a sharper 25-degree angle, the 4-ft flat bench width provides improved vehicle stability for both the passenger car and pickup truck.

Table 5.3. Evaluation Summary for SRGS with Different Flat Bench Section Widths under Modified Test 3-32 and 3-33 with 25-Degree Impact Angle

		Test 3-32, 25-Degrees, 2-ft	**Test 3-32, 25-Degrees, 4-ft**	**Test 3-33, 25-Degrees, 2-ft**	**Test 3-33, 25-Degrees, 4-ft**
Occupant Impact Velocity (ft/s)	X	39.5	39.9	28.2	28.2
	Y	1.7	0.4	3.5	4.3
Ridedown Acceleration (g)	X	12.0	13.8	9.5	11.5
	Y	6.0	5.7	6.5	6.2
Max. Angle (degrees)	Roll	19.5	11.2	7.6	11.2
	Pitch	16.0	9.0	43.9	31.5
	Yaw	11.2	4.7	40.4	42.5

Based on the simulation results, the modified SRGS design with a 4-ft flat bench width behind posts is recommended for full-scale crash testing. The extended flat section notably improved vehicle stability when compared to the original configuration with a 2-ft flat bench width. The evaluation also confirmed that a 25-degree impact angle is more critical than a 15-degree angle for the SRGS by producing more demanding vehicle responses. Therefore, this study recommends proceeding with two specific crash tests: modified MASH Test 3-32 (passenger car) and modified Test 3-33 (pickup truck), both conducted at a 25-degree impact angle at the center of the nose.

The simulation of modified Test 3-32 with the passenger car indicates a marginal performance outcome that is primarily due to a high OIV that approaches the MASH limit. This elevates the importance of physical crash testing to verify occupant risk. Another significant concern applicable to both Tests 3-32 and 3-33 is the high potential for rail rupture. This risk is substantiated by observations from prior physical tests in the NCHRP 15-53 project [2, 3] where rail rupture occurred. It is critical to note that the FE model used in this study does not include a rail rupture failure criterion. Consequently, the actual performance in a full-scale test could be more severe than what was simulated when taking into account possible rail rupture, therefore, making physical validation of the system's structural integrity essential.

A third test, Test 3-35 (redirection on the primary road), is not recommended. This is based on results from FOIL Test 20008 [2, 3], where the SRGS exhibited minimal damage and deflection (the maximum dynamic deflection was 18.7 in.) in a comparable redirection scenario. Since the only modification to the proposed design is extending to a 4-ft flat bench width, which does not alter core system components, the modification will not significantly impact the system’s stiffness or dynamic response in a redirection test.

While the simulation results from this study offer valuable insights into the predicted performance of the various design modification options, it is important to note that there is a key limitation of the finite element (FE) model used. The FE model does not explicitly capture rail rupture or tearing observed in NCHRP 15-53 project crash testing. In physical crash tests, rail rupture is usually initiated by a small, localized tear at the edge of rail, which then suddenly propagates through the entire rail section. Because the FE model does not incorporate specific failure for material fracture, it cannot replicate the rupture initiation and propagation behavior. Instead, the model assumes that the rail maintains continuous geometric integrity throughout the entire impact event. Consequently, the model cannot directly represent the physical rail breaking or tearing open under severe loading conditions.

Because the model preserves rail continuity and cannot capture the sudden propagation of a tear across the rail section, it also fails to simulate the system post-rupture behavior including the rapid loss of rail capacity, changes in system deformation, or the sudden redistribution of loads to the upper and lower cables in the system that would occur in reality. This limitation means the simulated responses may underestimate the potential safety implications associated with a physical rupture. Therefore, while simulations have been used in a manner to determine the design modification option with the best chance of success, full-scale physical crash testing remains essential. Given the complexity of the system and the model's inability to capture post-rupture dynamics, physical crash testing is necessary to validate the design and ensure the integrity and effectiveness of the containment system under actual testing conditions.

REFERENCES

1. American Association of State Highway and Transportation Officials. (2016). *Manual for assessing safety hardware* (2nd ed.). AASHTO.
2. Powers, R., Boodlal, K., Durkos, J., Boodlal, L., Marzougui, D., Kan, C. D., Opiela, K., & Tahan, F. (2022). *Roadside barrier designs near bridge rail ends with restricted rights-of-way: A guide*. The National Academies Press. https://doi.org/10.17226/26801
3. Powers, R., Boodlal, K., Durkos, J., Boodlal, L., Marzougui, D., Kan, C. D., Opiela, K., & Tahan, F. (2022). *Roadside barrier designs near bridge rail ends with restricted rights-of-way: A national survey and testing reports*. Transportation Research Board. https://doi.org/10.17226/26800
4. Abu-Odeh, A. Y., Mitchell, C., Bligh, R. P., Menges, W. L., and Kuhn, D. L. *Crash Testing and Evaluation of the TxDOT Short-Span Short-Radius Guardrail System*. Report No. FHWA/TX-17/9-1002-15-9. Texas A&M Transportation Institute, College Station, TX, January 2018. https://static.tti.tamu.edu/tti.tamu.edu/documents/9-1002-15-9.pdf
5. Abu-Odeh, A. (2025). *Proving ground simulation evaluation of a variation of the short radius system*. Texas A&M Transportation Institute Proving Ground. https://www.roadsidepooledfund.org/wp-content/uploads/2025/02/TRNo.604661-00001-Final.pdf
6. Roadside Safety Pooled Fund. (n.d.). *Phase I MASH testing of a thrie beam bullnose with breakaway steel posts (Test Nos. MSPBN-1, -2, and -3)*. Retrieved November 14, 2025, from https://www.roadsidepooledfund.org/longitudinal-barrier/phase-i-mash-testing-of-a-thrie-beam-bullnose-with-breakaway-steel-posts-test-nos-mspbn-1-2-and-3/
7. Roadside Safety Pooled Fund. (n.d.). *MASH testing of bullnose with breakaway steel posts (Test Nos. MSPBN-4 through MSPBN-8)*. Retrieved November 14, 2025, from https://www.roadsidepooledfund.org/longitudinal-barrier/mash-testing-of-bullnose-with-breakaway-steel-posts-test-nos-mspbn-4-through-mspbn-8/
8. Center for Collision Safety & Analysis. (2022). *2018 Dodge Ram 1500 FE coarse mesh model v3 – Validation* [Presentation]. https://doi.org/10.13021/4p7w-a040
9. Center for Collision Safety & Analysis. (2016). *2010 Toyota Yaris finite element model validation coarse mesh*. https://doi.org/10.13021/G8JS5D
10. Texas A&M Transportation Institute. *Test Risk Assessment Program (TRAP) [Version 2.5.2].* Retrieved from https://github.com/ttitamu/TRAP. 2024.